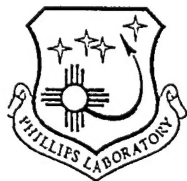

**REPETITIVELY PULSED, 70 JOULE PHOTOLYTIC
IODINE LASER with EXCELLENT OPTICAL and
LONG / RELIABLE OPERATION**

L.A. Schlie, R.D. Rathge

August 1996

Final Report

APPROVED FOR PUBLIC RELEASE; DISTRIBUTION IS UNLIMITED.



PHILLIPS LABORATORY
Laser and Imaging Directorate
AIR FORCE MATERIEL COMMAND
KIRTLAND AIR FORCE BASE, NM 87117-5776

19970325 028

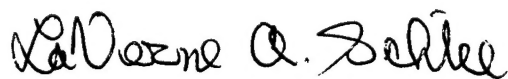
Using Government drawings, specifications, or other data included in this document for any purpose other than Government procurement does not in any way obligate the U.S. Government. The fact that the Government formulated or supplied the drawings, specifications, or other data, does not license the holder or any other person or corporation; or convey any rights or permission to manufacture, use, or sell any patented invention that may relate to them.

This report has been reviewed by the Public Affairs Office and is releasable to the National Technical Information Service (NTIS). At NTIS, it will be available to the general public, including foreign nationals.

If you change your address, wish to be removed from this mailing list, or your organization no longer employs the addressee, please notify PL/LIDD, 3550 Aberdeen Ave SE, Kirtland AFB, NM 87117-5776.

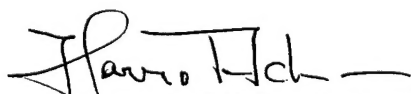
Do not return copies of this report unless contractual obligations or notice on a specific document requires its return.

This report has been approved for publication.

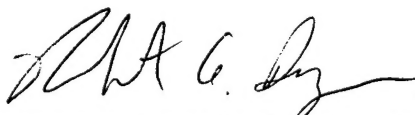


LAVERNE A. SCHLIE
Project Manager

FOR THE COMMANDER



HARRO ACKERMANN, GS-13
Chief, Laser Systems Branch



ROBERT A. DURYEA, Col, USAF
Director, Lasers and Imaging Directorate

1. Report Date (dd-mm-yy) August 1996		2. Report Type Final		3. Dates covered (from... to) 04 Mar 94 - 4 Oct 94	
4. Title & subtitle REPETITIVELY PULSED, 70 JOULE PHOTOLYTIC IODINE LASER with EXCELLENT OPTICAL AND LONG /RELIABLE OPERATION				5a. Contract or Grant #	
				5b. Program Element # 61102F/62601F	
6. Author(s) L. A. Schlie R. D. Rathge				5c. Project # 3647/3326	
				5d. Task # LA/LB	
				5e. Work Unit # 04/01	
7. Performing Organization Name & Address Laser and Imaging Directorate Phillips Laboratory 3550 Aberdeen Ave, SE Kirtland AFB, NM 87117-5776				8. Performing Organization Report # PL-TR-96-1046	
9. Sponsoring/Monitoring Agency Name & Address				10. Monitor Acronym	
				11. Monitor Report #	
12. Distribution/Availability Statement APPROVED FOR PUBLIC RELEASE; DISTRIBUTION IS UNLIMITED					
13. Supplementary Notes Supported in part by the Air Force Office of Scientific Research (AFOSR), Bolling AFB, Washinton, DC					
14. Abstract The performance of repetitively pulsed, 70 joule, closed cycle 1.3 uM photolytic atomic iodine laser with excellent beam quality (BQ = 1.15) is presented. This BQ was exhibited in the fundamental mode from a M = 3.1 confocal unstable resonator at a 0.5 Hz repetition rate. A closed cycle scrubber/laser fuel system consisting of a condensative-evaporative section, two Cu wool 12 reactor regions, and an internal turbo-blower enabled the laser to operate very reliably with low maintenance. The fuel system provided C3F7I gas at 10-60 torr absent of the photolytic quenching by-product I2. Using a turbo-molecular blower longitudinal flow velocities greater than 10 m/s were achieved through the 150 cm long by 7.5 x 7.5 cm2 cross sectional photolytic iodine gain region. In addition to the high laser output and excellent BQ, the resulting 8-12 usec laser pulse had a coherence length greater than 45 meters and polarization extinction ratio better than 100:1. Projections from this pulsed photolytic atomic iodine laser technology to laser energies, higher repetition rates, and variable pulse widths are discussed.					
15. Subject Terms iodine laser, photolytic pumping, closed cycle scrubber					
Security Classification of			19. Limitation of Abstract Unlimited	20. # of Pages 50	21. Responsible Person (Name and Telephone #) L. A. Schlie COMM: 505-853-3440 DSN: 263-3440
16. Report UNCLASSIFIED	17. Abstract UNCLASS	18. This Page UNCLASSIFIED			

ACKNOWLEDGMENTS

The authors would like to express their sincere thanks to the outstanding technical assistant Mr. J. Baker, R. Hagenloh, D. Stalnaker, and R. Wilmot in testing and construction of this laser is cited. Next, the synthesis efforts and technical interchanges of Mr. E. Dunkle and S. Herrera cannot be overlooked. Finally, the extensive technical interactions with Drs. G. Black, C. Clayton, A. Gavrielides, G. Hager, D. Mansel, and T. Walker are greatly appreciated along with the initial motivation of Dr. P. Avizonis.

TABLE OF CONTENTS

I. INTRODUCTION	1
II. PHYSICS OF REPETITIVELY PULSED PHOTOLYTIC IODINE LASER.....	1
III. EXPERIMENTAL DESCRIPTION	4
IV. RESULTS AND DISCUSSION.....	10
V. PROJECTION FOR HIGHER PULSED ENERGIES AND REPETITION RATES.....	13
VI. CONCLUSIONS.....	13
LIST OF REFERENCES.....	33

LIST OF FIGURES

ATOMIC IODINE SPECTROSCOPY	14
PHOTOLYTIC PROCESSES	15
PULSED PIL DEVICE	16
I ₂ REMOVAL SYSTEM/TURBO-MOLECULAR PUMP	17
PULSED FLASHLAMP CIRCUITRY	18
UV FLASHLAMP TRANSMISSION	19
VAPOR PRESSURES	20
INTEGRATED LASER BEAM DIAGNOSTICS	21
DETAILED LASER BEAM DIAGNOSTICS	22
LASER ENERGY VS PRESSURE (STABLE ENERGY)	23
LASER ENERGY VS OUTPUT COUPLING (STABLE RESONATOR)	24
LASER PULSEWIDTH VS OUTPUT COUPLING	25
LASER ENERGY VS PRESSURE (UNSTABLE RESONATOR)	26
LASER TEMPORAL BEHAVIOR RELATION TO FLASHLAMP CURRENT	27
SMALL SIGNAL GAIN	28

LIST OF TABLES

Table I: Atomic Iodine Hyperfine Transition Characteristics

Table II: Mean Free Path Lengths For Various Pressures of $\text{C}_3\text{F}_7\text{I}$

Table III: Critical Kinetic Processes for Pulsed Iodine Laser at $1.315\ \mu\text{M}$

I. INTRODUCTION

Recently, there has been much progress in the development of photolytic atomic iodine 1.315 microns lasers. Germany's Asterix IV pulsed Photolytic Iodine Laser (hereafter PIL) routinely produces single shot energies of 1.0 kilojoule in less than 1 nsec giving terawatt power levels.¹⁻⁷ Other scientists have also reported very good performance using explosively compressed inert gas flashlamps.⁸⁻⁹ In addition, research on cw PIL at 1.315 microns has demonstrated remarkable progress.¹⁰⁻¹⁴ In this article, a repetitively pulsed photolytic iodine laser operating in the closed cycle mode is reported which exhibits excellent optical properties and long/reliable operation. Pulsed energies greater than 70 joules per pulse at 0.5 Hz have been obtained in the lowest order unstable confocal resonator mode along with a long coherence length, excellent beam quality, and good polarization extinction. This photolytic iodine laser technology has been advanced to a simple and reliable operation using an I₂ removing scrubber flow system.¹⁵⁻¹⁷ In the subsequent sections, the physics of pulsed PIL's are discussed followed by a description of the laser device and its operating performance. Finally, the projection of the pulsed iodine laser technology for larger energies, higher repetition rates, and variable pulse widths are presented.

II. PHYSICS of REPETITIVELY PULSED PHOTOLYTIC IODINE LASER

The physical parameters critical to the operation of a repetitively pulsed PIL with excellent optical properties and long/reliable operation deal with the atomic iodine laser's hyperfine spectroscopy and broadening, photolytic excitation, atomic and molecular kinetics, and iodine gain medium's refractivity. A long coherence length (L_c) in the PIL depends on the oscillating hyperfine iodine transitions, the broadening mechanism, and resultant iodine spectral gain profile. Figs. 1-a/b illustrate the atomic iodine hyperfine splitting for both the ground and first excited states resulting in six hyperfine transitions governed by the selection rules $\Delta F = 0, \pm 1$ with $F' = 0 \rightarrow F'' = 0$ not allowed.¹⁸⁻²² The dominant transition is $F' = 3$ to $F'' = 4$ and Table I lists the wavelengths of each transition cited plus their A-coefficients.^{23,24} These six iodine hyperfine transitions have a significant effect on the coherence length of atomic iodine lasers since the coherence length varies inversely with the linewidth. Consequently, the number of oscillating hyperfine transitions is important.^{25,26} A coherence length L_c equates to $c/\Delta\nu$ or $1/\Delta k$ where c is the velocity of light, $\Delta\nu$ is the total linewidth of the laser spectrum, and Δk is the corresponding wave number difference. If all six of the iodine hyperfine transitions existed in the laser output, then $\Delta k = 0.725 \text{ cm}^{-1}$ giving a small coherence length of 1.37 cm. For simplicity, only the line center Δk values are used. With only the two highest gain hyperfine transitions, $F' = 3 \rightarrow F'' = 4$ and $2 \rightarrow 2$ oscillating, $\Delta k = 0.453 \text{ cm}^{-1}$ yielding a laser coherence length of 2.21 cm. This simple

analysis shows long coherence lengths will *exist only if one hyperfine transition oscillates*. Even with only one hyperfine transition lasing, a significant decrease in the iodine laser's coherence length will still occur if two or more longitudinal modes are oscillating. With the unstable mirror spacing at 2.84 meters (Sect. III), a $c/2L$ value 52.8 MHz results corresponding to a coherence length $L_c = 5.68$ meters. The Doppler broadened line width is 240 MHz (FWHM) at room temperature²⁷ and thus more than one longitudinal mode is possible since $g_o L$ values greater than one exists in the PIL gain medium (Sect. IV). Sect. IV also relates the optimum operating pressure of C_3F_7I is 30-45 torr. For this pressure range, the large 20 MHz/torr broadening coefficient²⁸⁻³¹ of C_3F_7I causes the iodine gain medium to be homogeneously broadened with line widths of 600 to 900 MHz. Calculated gain profiles shown in Fig. 1-c/e illustrate the overlapping of these hyperfine transitions as a function of C_3F_7I pressure.²⁷ The resulting oscillating frequency would be expected to be very close to the $F' = 3$ to $F'' = 4$ hyperfine transition since a homogeneously broadened transition lases near line center.³² In addition, this laser transition should oscillate in only one longitudinal mode with a very narrow linewidth resulting in a long coherence length. This effect is believed to be responsible for the L_c values greater than 200 meters observed in a cw photolytic iodine laser and the large values reported below for pulsed PIL's.³³

240-320 nm UV (ultraviolet) radiation photolytically dissociates $n-C_3F_7I$ (normal form and hereafter, C_3F_7I) into an excited iodine $5^2P_{1/2}$ atom and a free $n-C_3F_7$ radical specie with nearly 100% quantum yield.³⁴ Fig. 2-a shows the associated photolytic cross section. Using a mean cross section (σ_p) of $4 \times 10^{-19} \text{ cm}^2$ provides a good estimate for the UV radiation's mean free path lengths $l_p (= 1/\sigma_p N)$ listed in Table II with N representing the C_3F_7I density. A square physical geometry having excitation from 2 or more sides acquire near uniform pumping when the width $d \cong 4 l_p$. A uniform near-field laser beam profile in the lowest order mode from a confocal, unstable resonator was observed for C_3F_7I pressures of 30-45 torr when the $7.5 \times 7.5 \text{ cm}^2$ cross section was excited on opposite sides (Sect. IV). The corresponding l_p is 2.56-1.70 cm for this pressure range which is approximately $d/4$. The flashlamp's UV intensity *was not sufficient* to create bleaching effects often observed with very intense UV sources.^{35,36} Approximately 1% of the C_3F_7I was photolyzed into excited I^* and C_3F_7 . Simple analysis of the flashlamp output provides valuable insight into the operation of pulsed PIL's. Later results will show typical mean input powers deposited into the flashlamps to be approximately 100 MW during a 10 μsec current pulse. For the 1 cm i.d., 80 cm length, 150 torr xenon filled flashlamps excited with 3.7 μf capacitor charged to 30 KV, this approximate mean power would result in an output intensity of 400 KW/cm² over all wavelengths if all the lamp deposited energy was radiated. Using a nominal UV conversion efficiency of 2% yields an approximate peak intensity of 8 KW/cm² which corresponds to a fluence of 1.6×10^{22} photons/cm²·sec at the 272 nm C_3F_7I peak cross section.

Assuming a 10 μ sec flashlamp UV radiation square pulse and taking 30 torr of C_3F_7I in the gain region, a peak excited iodine density of $4 \times 10^{16}/cm^3$ can be produced using the mean photolytic cross section of $4 \times 10^{-19} cm^2$. With a stimulated emission cross section (σ_{se}) value of $5 \times 10^{-18} cm^2$ (Ref. 27), this excited iodine density corresponds to a maximum unsaturated small signal gain coefficient of 20% / cm which is close to the measured values of Sect. IV. This simple analysis also indicates that about 1% of the C_3F_7I laser fuel is being excited which enables the closed cycle, I_2 removal system scrubber to operate successfully.

Once the C_3F_7I molecules are photolyzed, various kinetic processes occur in the iodine gain medium as listed in Table III. Some processes are included to emphasize the C_3F_7I laser fuel purity requirements. Temperature dependent rates which play a significant role in the overall kinetics are not included but are discussed elsewhere.³⁵⁻³⁷ No buffer gas was used to simplify the operation of the closed cycle, laser "fuel" system (Sect. III) and minimize optical-gas medium disturbances. Pulsed photolytic atomic iodine lasers have always been easy to demonstrate due to high peak ultraviolet radiation generated from flashlamps.⁴⁸⁻⁵⁴ The extractable energy, however, can vary significantly due to impurities and the photolytic by-product I_2 . Elimination of O_2 , H_2O , and I_2 is essential to minimize these excited iodine quenching processes with the result being higher energies along with earlier onset of lasing relative to the flashlamp's initiation. In the absence of such impurities, only two quenching processes for the excited $5-^2P_{1/2} (I^*)$ iodine atoms dominate, namely



which have rate constants of 7.9×10^{-13} and $2.8 \times 10^{-16} cm^3 \cdot sec^{-1}$, respectively.³⁷⁻⁴¹ I represents the ground state of atomic iodine. Above, it was related that excited iodine density of $10^{16}/cm^3$ can exist in the iodine gain mediums. For this density, the I^* loss rates are respectively 7900 and 274 sec^{-1} which are negligible during a 10 μ sec laser pulse. Similar analysis for O_2 , H_2O and N_2 impurities show for pressures less than microns ($< 10^{13}/cm^3$), negligible I^* quenching occurs. The most important I^* quenching process is by the photolytic by-product I_2 , namely



which has a large quenching rate constant, approximately $10^{-11} cm^3 \cdot sec^{-1}$ (Refs. 42-43). The production of I_2 increases during and after the photolytic UV pumping pulse because I_2 is a by-

product of the irreversible recombination channel of the photolyzed C_3F_7I . There exists a small dissociation of I_2 by 500 nm radiation,⁵⁵ but it is too small to eliminate this photolytic by-product. At the maximum C_3F_7I pressure of 60 torr used, the concentration of C_3F_7I is $1.96 \times 10^{18}/cm^3$. Again using an approximate I^* and I density of $10^{16}/cm^3$ in process (11) of Table III, the 3-body formation rate by C_3F_7I becomes $7.5 \times 10^3 \text{ sec}^{-1}$ or $1/134 \text{ } \mu\text{sec}$. Therefore, during lasing no significant excited iodine quenching by I_2 should occur but an I_2 density in excess of $10^{14}/cm^3$ can result 10's milliseconds after the UV excitation pulse. Consequently, its removal by the closed cycle flow system (Sect. III) is crucial for repetitively pulse operation.

Important to all lasers is the effect of gain medium density fluctuations on the quality of the output laser beam. The ability to obtain a near diffraction-limited optical beam depends on the magnitudes of two parameters; namely, the spatial variation of the gain medium's gas density fluctuations $\Delta N/N$ or $(N - N_0)/N$ variation and the polarizability α (accounted for by the refractivity Δn) of the individual gaseous species present. Here, N_0 denotes the equilibrium density. $\Delta n = 2\pi\alpha N$ where N equals the total number density of the gas being examined. For C_3F_7I , $\alpha = 1.16 \times 10^{-23} \text{ cm}^3/\text{molecule}$ at 1.315 microns while for I_2 $\alpha = 1.25 \times 10^{-23}$. (Ref. 56) The magnitude of the non-constant cross-sectional phase shift difference, $\Delta\phi$, an optical beam experiences while propagating through a medium of length L with spatially varying density is

$$\Delta\phi = \frac{2\pi}{\lambda} \alpha (N - N_0) L \quad (4)$$

Taking a maximum single pass phase shift across the gain media less than 1/10 wave over the 150 cm gain length reported below, Eqn. (4) relates $\Delta N/N_0$ must be less than $1.75 - 2.6 \times 10^{-3}$. Using the optimum C_3F_7I pressure of 30-45 torr also reported below, such a requirement is easily established and is consistent with the excellent unstable beam quality reported below. Since there was no requirement to have buffer gas in the photolytic iodine laser, its operation at relatively low pressure minimized optical medium disturbances.

III. EXPERIMENTAL DESCRIPTION

Figs. 3 and 4 show the schematic of this pulsed photolytic iodine laser device. The two iodine gain cells are 125 cm long, 7.5 cm square gain cells each having 7.5 cm x 80 cm, 2.5 cm thick, commercially polished fused silica transmissive UV windows on opposite sides. Individual gain cells were used due to fabrication easy and availability of the UV windows. These windows obtained from Corning Glass are 7940 commercial Grade F with inclusion Grade 3 and were free of OH radical to minimize the formation of color centers. Such color centers can produce significant transient UV absorption.⁵⁷ These UV quartz windows were vacuum sealed with Viton

rubber O-rings assuring minimal stress and good vacuum integrity. Three equally spaced pulsed Xe flashlamps were mounted above each of these UV windows. There were a total of twelve lamps exciting the 8.4 liter laser gain region and the gain cells were fabricated with T6061 aluminum due to its good chemical compatability with the C_3F_7I . At each ends of the gain cells are the unstable resonator mirrors plus at one end, a 45° polarizing reflector. For the stable resonator tests (Rigrod analysis) and iodine gain medium interferometric diagnostics, the internally mounted mirror mounts were replaced with 1.315 μM , AR (anti-reflection, $<1\%$) coated 2.5 cm thick, $\lambda/10$ at 632.8 nm, 6 inch diameter BK-7 glass windows. To eliminate parasitic oscillations due to the large integrated gains existing in the iodine gain cell, the internal walls were bead blasted with 10 mesh Al_2O_3 "chunks" to create a 60-100 mesh equivalent surface texture and a 50 mil high, octagon "fence" was placed on the UV window surfaces. In addition, no internal optical elements such as AR coated windows were possible.

The Xe flashlamps were 1 cm i.d., 1 mm wall thickness, low alkali clear quartz filled with 150 torr of pure xenon gas and acquired from ILC Corp.⁵⁸ The lamp electrodes were insulated to 40 KV using a silicon sealed coaxial cylindrical tube surrounding the cable/electrode connector. Bored teflon spheres used to mount these flashlamps allowed them to expand or vibrate during repetitive operation. Each flashlamp was excited with separate 3.7 μF capacitors charged to 15-30 KV and switched with a single, modified Maxwell spark gap (SG), M/N 40359 shown in Fig. 5. A Maxwell Trigger Generator 40230 (-100 KV pulse) was used to trigger this mid-plane spark gap switching all of the twelve lamps simultaneously. To achieve reliable operation the SG was operated in the recommended "irradiated triggering mode" configuration and the power supply was connected to this spark gap through a 10 $M\Omega$ resistor (R_{sg}) to assure complete ionization of the spark gap during its triggering. The temporal behavior of the flashlamp's currents were monitored using Pearson current transformer M/N 1025 coupled to a Tektronix 11401 digitizing oscilloscope. Each capacitor was connected to a high voltage through a normally closed remote controlled shorting switch connected to the safety interlock of the ALE Systems, Inc. power supply M/N 302L "master" with five M/N 302S "slaves". Since one of the intents of this effort was to acquire short pulsewidth near 10 μ sec, it was necessary to excite the flashlamps at very high power levels in excess of 300 MW with peak plasmas deposited energies greater than 1.7 Kjoules. At these high energies, the flashlamp lifetime (shots before destructively failing) becomes quite short.⁴⁸⁻⁵⁴ Another issue was the O_3 absorption which very closely overlaps the C_3F_7I photolytic absorption band as seen by comparing Figs. 2-a and -b.^{59,60} The formation of most of the ozone occurred after the flashlamp pulse and thus air convection was necessary for its removal. Analysis of the ratio of the lamp's deposited discharge E_o energy (1.71 KJ) to its explosion energy E_x (4.82 KJ) gives 0.34 indicating the lamp should last less than 10^4 shots.⁴⁷⁻⁵³ For repetitive operation, this condition was marginally acceptable and thus some type of

convective cooling was essential. Air, pure N_2 , and water cooling were examined for the cooling of these flashlamps. Cooling with air resulted in small ($< 10\%$) reduction in laser energy attributed to transient build-up and residual ozone production between pulses.⁵⁸ With N_2 , no decrease was observed. Water cooling commonly used in flashlamp pumping of solid state lasers was anticipated to be attractive because of its higher heat capacity, minimization of flashlamp vibrations/breakage, and negligible acoustical noise. With coaxial water cooling of the flashlamps, 50% reduction in the laser energy occurred. This decrease was attributed a decrease in the UV transmission through the water. Use of titanium doped fused quartz in place of the low alkali fused quartz was an improvement ($\cong 15\%$) but still significantly lower than with N_2 gas cooling. Fig. 6 shows Ti doped quartz eliminates all UV radiation below 220 nm. The transmission difference between the two different quartz suggests absence of lower wavelength UV radiation may minimize production of transient UV absorbing species in the water. Regardless what the mechanism may be, no water cooling approach seemed acceptable. Flat reflectors behind the flashlamps were used to enhance the UV radiation into the iodine gain region giving small improvements. Different types of coatings were placed on these flats with $BaSO_4$ being the best.⁶¹

Previously, a completely passive closed-cycle flowing alkyl-iodide (C_3F_7I) gaseous supply system was reported.^{15,16} This system provided a high purity and fixed pressure of gaseous C_3F_7I with virtually unlimited operating time, but the resultant flow velocity (1-2 m/s) was too low for the required greater than 10 m/s. To fulfill this need, a scaled-up version of the I_2 removal scrubber system was used coupled with an oil-free turbo-molecular blower as shown in Fig. 4. C_3F_7I gas has unique physical properties suitable for use in a closed cycle flowing system with simultaneous "scrubbing" or removal of the photolytic by-product I_2 . It is a clear liquid with a freezing point of $-78^\circ C$ and the property of turning purple with dissolved I_2 .^{15,16} Fig. 7-a gives the vapor pressure. Typical operating pressures of the pulsed photolytic iodine laser are 20-60 torr correlating to temperatures of -35 to $-18^\circ C$ for the condensative-evaporative closed-cycle flow system. H_2O , O_2 , and the photolytic by-product I_2 are strong quenchers of the excited iodine atoms and consequently their removal is essential. The molecular iodine and water vapor pressure curves, Fig. 7-b, indicate that both I_2 and H_2O have negligible vapor pressures for the sub-zero operating temperatures and thus pure laser fuel at a fixed pressure can be produced unless the solution becomes saturated with molecular iodine. To assure clean C_3F_7I laser "fuel" is initially used, 99% pure C_3F_7I is acquired using a specific synthesis/distillation process.¹⁷ I_2 is initially removed by pouring the C_3F_7I through Cu wool several times and the removal of O_2 and N_2 dissolved in this alkyl-iodide was done via a LN_2 freeze/thaw method.^{15,16} The scaled sized, closed-cycle, C_3F_7I chemical scrubber system (Fig. 4) was an integration of the turbo-molecular blower with the condensation and evaporation sections of the previous passive flow system. Each

of these two sections were cooled to different temperatures and coupled with a stainless steel (s.s.) tube. All components were made of stainless steel to minimize temperature drifts and both the condensative and evaporative sections were encased in insulated jackets to reduce heat transfer. The quantity of liquid C_3F_7I was sufficient to assure its liquid level was above the 1" ss tubing connection between the condensation and evaporation cells. Approximately 1 Kg of C_3F_7I was sufficient to sustain reliable lasing for several weeks. This liquid filling isolated the two cells and forced gaseous C_3F_7I to flow from the evaporation to the condensation zone via the laser gain cell even without the blower. The condenser section (Fig. 4-a) consists of a 0.5" diameter ss 304 tubing wound in a 3" diameter helical coil through which cooled (-40 to -60 °C) denatured alcohol is circulated via a Neslab ULT 80 cooler. This coil is enclosed in a 4" diameter tank packed in fine copper. When the C_3F_7I/I_2 solution passed through the fine copper wool, most of the I_2 was removed by reaction with the Cu wool forming CuI .⁶² The remaining I_2 still not removed is then deposited as either a solid or dissolved in the liquid C_3F_7I . On the right side of Fig. 4-a is the evaporative region retained at temperature greater than the condensative from which clean C_3F_7I is liberated with negligible I_2 vapor. This evaporative section's temperature was established by a 5 inch long s.s. coil similar to that in the condensative section. The evaporative coil was covered with Al beads to increase heat conduction to the liquid C_3F_7I . Again, denatured alcohol controlled by a Neslab cooler LT-50 at temperatures of -30 to -15°C was used. Any residual I_2 vapor is reacted with the Cu wool placed above the evaporative coil of the scrubber system. An analysis of the cooling power required to condense all of the C_3F_7I to remove the molecular by-product I_2 provides very valuable information. To evaluate maximum requirements, take a flow velocity of 10 m/s and a maximum operating pressure of 60 torr C_3F_7I through the 4" diameter piping (Fig. 4-b). The volumetric flow velocity becomes $8.1 \times 10^4 \text{ cm}^3/\text{sec}$. This value results in a C_3F_7I mass density flow rate of 76.98 g/sec or 0.26 moles/sec. Using the enthalpy ($H_v = 24.3 \text{ KJ/mole}$)^{15,16} of C_3F_7I indicates that a maximum 6.4 KW is required to condense all of the C_3F_7I . A modification of this closed cycle system allowing some of the laser "fuel" to bypass the condensative section will reduce the cooling requirements. Such a procedure may be practical since low densities of molecular iodine are produced during photolysis. To produce flow velocities greater than 10 m/s while operating at relatively low pressures of 20-60 torr, a special blower was required due to the massive C_3F_7I molecule (296 amu). Various non-contaminating blowers were initially examined such as piston drives and centrifugal, but none of these pumps could simultaneously produce the flow velocity and sustained operation with this heavy molecule without contaminating the C_3F_7I . A modified turbo-molecular pump provided the flow velocity and sustained operational requirement. The turbo-molecular blower (TMB) was originally an Airco Corp. M/N 1514 operating at 20,000 rpm. Details of this turbo-molecular blower (TMB) are described elsewhere.⁶³ Large pressure compressions are obtained by using wedged rotors

concentric with similar stators as shown and rotating the well balanced rotors blades at 2-3000 rpm. The resulting pressure compression of (10-100) creates a large enough pressure head that high flow velocity results. A Ferrofluidic M/N SC-1000-C rotating vacuum seal provided the non-oil contaminated, vacuum environment.^{64,65} At the bottom compression side of the blower, Fig. 4-b shows two exit ports which provide C_3F_7I at flow velocities greater than 10 m/s to both ends of the iodine gain cells. The flow velocities were initially measured using a 1 inch Vortex flow meter, M/N YF102.

Both stable and unstable resonators were used in understanding the performance of this pulsed photolytic iodine laser. The Rigrod gain-saturation curves obtained with a stable, hemispherical resonator with AR coated flat windows were used to establish the optimum magnification for the confocal, unstable resonator.⁶⁶⁻⁶⁹ This stable resonator had a maximum reflectivity, 10 meter radius of curvature, 6" diameter mirror and flats with transmissions of 10, 20, 30, 40, 50, 60, 70, 80, and 100%. Nominal mirror spacing was 2.6 meters. It is beneficial to note that 1.315 μ M coated mirrors also have high reflectivities at wavelengths between 420-460 nm which made the 1.315 micron resonator mirror alignment easy with an Ar^+ 458.9 or $HeCd^+$ 441.6 nm. The unstable resonator was a positive branch, confocal type chosen to prevent any internal focus and its critical parameters are⁷⁰⁻⁷²

$$R_1 = \frac{2L}{1-M} \quad R_2 = \frac{2ML}{M+1} \quad (5)$$

where R_1 , R_2 , M , and L are respectively, the mirror radius of curvatures, the magnification $M (= |R_2|/|R_1|)$, and the mirror distance $L (= |R_1| - |R_2|)$. The geometrical equivalent output coupling $c_g = (M^2 - 1)/M^2$. The laser beam width was equal to the cavity width w with the small feedback aperture a related by $w = Ma$. The confocal unstable resonator shown in Fig. 3 has two distinct novelties. First, instead of the conventional scraper to couple laser energy from the resonator, transmissive coupling was incorporated. At 1.315 microns, the laser mirror substrates (BK7) have excellent transmissive properties. Such low absorption of laser radiation at this wavelength relates to negligible mirror heating and thus no noticeable aberrations are introduced by the output coupling mirror. The feedback mirror is a meniscus mirror; i.e., having different radii of curvature on the front and back surface. Both surfaces were convex and AR coated. The front surface consisted of an AR coating at 1.315 microns plus a square, maximum reflecting coating at 1.315 microns. This square reflecting coating was centered on the square 7.5×7.5 cm² iodine gain cell and had a width w such that the relation $Ma = 7.5$ cm was satisfied. Rigrod gain-saturation data and the transient laser pulse behavior of Sect. IV. shows an optimum 90% output coupling corresponding to a magnification $M = 3$. The mirror distance $L (= |R_1| - |R_2|)$ was required to be

2.85 meters. From the above confocal resonator relations, the two mirror radius of curvatures became -2.73 and 8.41 meters with a square feedback width of 2.35 cm. The exact magnification was 3.08. On the back side of the feedback meniscus mirror, the radius of curvature was -2.78 meters. This different radius of curvature accounted for the refractive index bending of the laser radiation as it propagated through the BK7 substrate assuring the laser output beam was collimated. To minimize any reflections from this surface, an AR coating was also deposited. The second novelty deals with the opposite end of the resonator where a 45° angle reflecting flat coated for maximum reflectivity of p-polarized radiation and less than 10% for s-polarization was placed. For round trip propagation, only p-polarized laser output was produced as shown in the next section. This last operation was necessary since an unstable resonator with no internal Brewster windows or turning flats has no polarization selectivity. The p-polarization coating on this flat mirror provided very good polarization extinction. The bellows on both ends of the gain cells allowed exact spacing control to assure collimated laser output plus allowing easy mirror alignment. These stainless steel mirror boxes used a double concentric screw adjust to insure negligible movement during repetitive laser operation. To align the internally mounted mirror of the unstable resonator, the approach originally established by Krupke and Sooy was followed.⁷³

Since the ultimate goal was to produce a repetitively pulsed iodine laser with excellent beam quality, large coherence length, good polarization extinction, and short pulse width (8-12 μ sec) while operating repetitively, several different optical diagnostics were performed on the laser output as shown in Figs. 8-9. All the diagnostics were placed on an air-floating optical isolation table and the electronic instrumentation was placed in a screen room. The laser pulsed energy and average power measurements were made using a Scientech M/N 380801 volume energy absorber. Transient laser behavior was monitored with a Judson germanium 500 Mhz photodiode M/N J16 observing either the small transmitted laser energy from the high reflector mirror of the stable resonator or 45° p-polarizing mirror of the unstable resonator. A 1 mm diameter quartz fiber optic placed on the edge of laser beam transmitted a fraction of the laser energy into a screen room. The resulting laser pulses were then recorded on a Tektronix 11401 digitizing oscilloscope along with the flashlamp current pulses. To perform the iodine gain measurements, a low power (few milliwatt), well stabilized cw atomic iodine laser was used.^{13,14} The iodine gain medium quality measurements were made using a standard Mach-Zehnder interferometer employing an Ar^+ at 514.5 nm.⁵⁶ Operating at this wavelength was critical due to the I_2 production during and after the photolytic UV excitation. Other Ar^+ laser transitions like 488 nm can experience complete absorption by the molecular by-product I_2 (Ref. 74). The resulting fringes were monitored both visually and with a Hamamatsu M/N C2741 camera sensitive from 400 nm to 2 μ M having 240 x 240 pixels in approximately 1 cm^2 . The output from this camera was processed

by a KSI time code annotator and then displayed and permanently recorded with a Panasonic VCR.

Fig. 9 shows the detailed laser diagnostics employed. To monitor the laser beam profiles from both the stable and unstable resonator operation of the iodine laser, two monitoring techniques were employed. The first method, mainly for quick observation, was a 10 inch square, Kodak thermal sensitive, phosphorescent IR screen which was sensitive to 1.315 micron radiation. It fluoresced for approximately a second after the laser pulse. Sometimes a UV blocking/1.315 micron transmissive filter was used to block the very intense visible light produced by the flashlamps. The second detecting technique was again the Hamamatsu camera system described above. This unit was also used in the coherence measurements. To obtain the beam quality measurements, two different Cassegrainian telescopes were used. A quartz optical wedge with mirror flatness ($\lambda/10$) was employed to provide 0.4% of the laser beam energy into the telescope. This thin quartz flat's mirror figure was critical since it could ultimately affect the resultant beam quality measurements. The output of each of these telescopes was then detected by the infrared camera and subsequently monitored. Such data was then analyzed to assess the laser beam quality as will be discussed in Sec. IV. The coherence length measurements were determined by demonstrating interference from a variable arm distance difference of a Michelson interferometer as previously described.⁵⁶ Finally, the polarization of the laser beam from the unstable resonator was determined using a double Brewster window combination, Fig. 9-d. Knowing the expected angular position of the polarized radiation, the Brewster window system was rotated to obtain the different transmission. Comparison with calculated transmission results determined the polarization nature of the laser beam.

IV. RESULTS AND DISCUSSION

Data on the overall performance of pulsed photolytic atomic iodine laser at 1.315 microns verifies its excellent beam quality, coherence length, and polarization optical qualities. In addition, the coupling of the closed cycle, I_2 removal scrubber system to the longitudinal flowing iodine gain medium worked very well with operation of more than two weeks using the same C_3F_7I "batch" of laser fuel. The design of an unstable resonator was established from the data of Figs. 10-12. Consistent with the mean free path distances of Table II, Fig. 10 relates that the maximum laser energy was obtained for 60 torr of C_3F_7I with a small change as this pressure varies from 30 to 70 torr. In addition, a fairly uniform spatial gain profile existed. Fig. 11 gives the gain-saturation curve for a pressure of 40 torr.⁶⁶⁻⁶⁹ Although there is some variation in this curve, no well defined peak for the optimum transmission exists. The transient pulse shape data of Fig. 12 and this laser energy versus transmission curve indicates that most of the energy can be

extracted from the iodine gain medium but just at a slower rate which correspond to longer pulsewidths. With impurity free C_3F_7I , the quenching loss for excited iodine atoms ($5^2P_{1/2}$) is very small thus allowing the gain to exist for nearly a millisecond after the UV excitation. Therefore, to obtain the optimum transmissive coupling, the laser pulse behavior should be made to closely overlap flashlamp current. For transmissive couplings near 90% the best overlap of the laser pulse to the flashlamp's current occurred. An equivalent unstable, confocal resonator geometrical coupling (c_G) corresponds to a magnification of 3.

Fig. 13 shows the extracted energy from this $M = 3$ unstable resonator shown in Fig. 3 versus the C_3F_7I pressure indicating the optimum pressure operation is 30 to 45 torr. The difference from the stable resonator results of Fig. 10 is attributed to a more uniform spatial gain profile created at the lower C_3F_7I pressures plus increasing the UV lamps from 8 to 12. The extractable laser energy is 8.3 joules/liter. Fig. 14 shows the resultant laser pulse shape relative to the flashlamp current transient behavior illustrating a delay of 3-4 μ sec before the onset of the laser pulse. Except for this delay caused by the transient build-up of UV radiation in the flashlamp, Fig. 2-c, and similarly the establishment of an iodine inversion, the laser pulse shape follows quite closely that of the current. The "noise features" on this laser signal are relaxation oscillations.⁷⁵ The near-field laser profiles are very flat ($< 5\%$ variation) with a square hole due to the feedback. The far-field data has a very strong central lobe and negligible side lobe intensity ($< 2\%$). These far-field laser beam profiles were obtained using the telescope shown in Figs. 8-9. The resultant BQ was determined comparing the normalized ratio of the integrated theoretical far field beam intensity (I_{theor}) versus radius to the experimental value (I_{expt}) which is often called "power in the bucket".⁷⁰⁻⁷³ The beam quality BQ is given by $[I_{theor}/I_{expt}]^{1/2}$. Performing such analysis far-field beam profiles at several different radial positions gave a BQ of 1.3 times diffraction limited. More refined techniques using the telescopes of Fig. 8-9 gave BQ measurements of $1.15 \times$ diffraction limited. This good beam quality is very understandable since the C_3F_7I pressure inside the laser gain cell is quite low. The collimation of the laser beam was then tested by propagating it approximately 100 meters. By varying the distance between the mirrors with the bellow assembly shown in Fig. 3, excellent collimation was easily obtained. With these excellent beam quality and collimation results, an experimental measurement of the pulse to pulse laser repeatability and average power were determined giving less than 5% variation in the laser output. Typical run times were five minutes.

Besides the recent coherence length measurements of the low power, cw photolytic iodine laser, there exist no other reported coherence length results for any other type of photolytic iodine laser.³³ A conventional Michelson interferometer was used to determine the coherence length with the existence of fringes monitored as the distance between the arms was varied using the infrared camera described previously. Interferometric fringes for arm length difference of 45

meters were easily detected. The resulting stable fringes clearly demonstrated the long coherence length of this photolytic iodine laser. This coherence length value indicates that only one hyperfine transition can exist. In Figs. 1-c/e, an analysis of the gain profiles for C_3F_7I pressures of 12.5-50 torr showed that these profiles overlap due to pressure broadening. Consequently, the results here also suggest it is reasonable to conclude that the iodine gain medium acts as a homogeneously broadened transition. Since only one longitudinal mode can lase in a homogeneously broadened transition, the observed coherence length is explainable. A much longer coherence length may exist, but the measurement is difficult requiring transient laser linewidth measurements. Using the double Brewster window, Fig. 9-d, the polarization of the laser beam was determined. By rotating this unit, the polarization was determined to have an extinction greater than 100:1.

To further understand the performance of this pulsed PIL, small signal gain data is shown in Fig. 15. These measurements were made through a path length of only 5 cm using a stable, 5 mw TEM_{00} atomic iodine photolytic iodine laser.^{13,14} The large small signal gains prevented longer gain length since the medium would lase even with only AR coated windows. Two valuable pieces of information can be interpreted from these gain measurements. First, the large values for the peak gains, 26.6 %/cm, are quite amazing. Such values are the reason parasitic control in the unstable resonator was quite difficult to achieve. Even with only 5 cm of gain length, g_0L products greater than 1 can be achieved. For the 150 cm gain length, a very large $g_0L = 39.9$ existed but parasitics were eliminated giving only the lowest order mode in the unstable resonator. Another feature of this gain data is that the gain has a few microsecond risetime before it reaches its maximum value. This build-up of gain is directly associated with the flashlamp's transient UV emission as Fig. 2-c illustrates.⁴⁸⁻⁵⁴ Lastly, this data shows that the iodine gain persists for a long time with only a small decrease from its peak value at the end of the flashlamp pulse. This condition enables most of the iodine medium's stored energy to be extracted even when a low output coupling fraction is used as Fig. 12 shows. During lasing these large peak gain values do not exist since the lasing strongly saturates the medium. Saturated gains obtained by going transverse to the lasing axis are a factor of 10 lower during lasing. The small undulation on the gain data for times greater than 100 μ sec is due to shock waves and for times greater than ca 750 μ sec, absorption at 1.315 microns is observed. Finally, laser interferometric measurements at 514.5 nm were made to assure the iodine gain medium was optically clear before another flashlamp pulse excited the medium. In less than one second after the flashlamp pulse, the medium was optically clean. Some heating effects from the UV window "fence" occur close to these window edges, but it has negligible effects on the far-field laser beam quality.

V. PROJECTION FOR HIGHER PULSED ENERGIES AND REPETITION RATES

With the excellent optical performance of this high energy, repetitively pulsed photolytic iodine laser at 1.315 micron, its projection to higher energies, shorter and longer pulsewidths, and higher repetition rates are possible. All the features such as the C_3F_7I scrubber system, turbo-molecular blower, and unstable resonator operation makes this system easily scaled. Using transverse flow to replace the longitudinal flow offers the possibilities of easily increasing the pulse rate to 10-20 Hz. Such a configuration would require upstream and downstream acoustical absorber to assure the lasing medium is optically clear to obtain good laser beam quality. Scaling the turbo-molecular pump to high flow velocities by simply increasing the rpm of the rotors should be very straightforward. The available energy in joules/liter could also be increased by exciting the gain mediums for much longer times. Since the gain in an iodine gain medium lasts for a long time after the UV flashlamp's excitation, much shorter pulses may be obtained using an electro-optical (E-O) switch.⁷⁶⁻⁸⁰ Care would have to be taken to deal with the possible onset of parasitic oscillation when such devices are inserted internal to an unstable resonator due to the large gain coefficients.

VI. CONCLUSIONS

The technology of pulsed, photolytic iodine lasers at 1.315 micron has demonstrated excellent optical qualities and reliable performance by using a 3.1 magnification, unstable confocal resonator to extract more than 70 joules of 1.315 micron radiation in the lowest order mode. Optical diagnostics of the laser beam relates its excellent beam quality less than 1.15 times diffraction limited with good collimation and polarization extinction plus a coherence length greater than 45 meters. Using the I_2 removal scrubber system and the internal turbo-molecular blower, long and reliable operation of this laser device was obtained. The projections of this laser to higher energies, pulse repetition rates, and powers are feasible. This type of photolytic iodine lasers can provide safe, reliable, compact, high power laser performance at 1.315 microns. In addition, the PIL's reliable operation, low fabrication and operating costs, and excellent beam quality makes them a very useful source of high energy, high power one micron radiation. Improvements in the present 0.25 to 0.5 % efficiency will occur with the use of alternate laser "fuels" and "tailored" flashlamps to the photolytic cross sections.

Atomic Iodine Spectroscopy

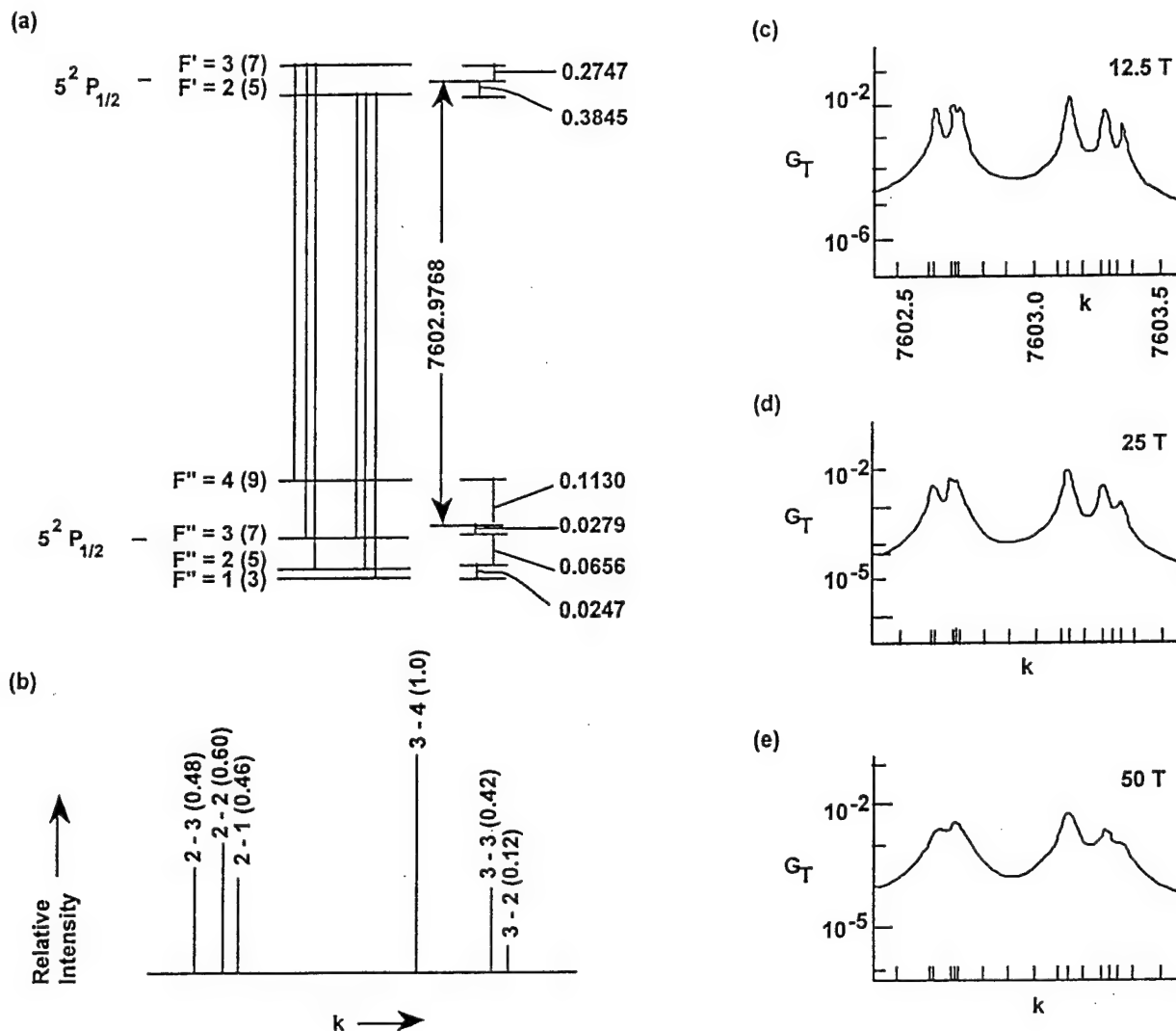


Fig. 1: Pertinent atomic iodine structural information, (a) hyperfine structure of atomic iodine as function of wave number k ($1/\lambda$) along with its associated transitions for $5-2P_{1/2}$ and $5-2P_{3/2}$ states, (b) relative intensities of hyperfine transitions. In (a), the number in parentheses is $g (= 2F + 1)$, the degeneracy of the iodine hyperfine level while in (b), the number in parentheses is the relative intensity level, and F denotes the quantum number. All energy spacings are given in inverse centimeters. (c) - (e) illustrate the sum of the calculated fractional gain (G_T) profiles for three different pressures of C_3F_7I assuming 20 MHz/torr broadening and an atomic iodine inversion density $[I^* - I/2]$ is $10^{16}/\text{cm}^3$ with (c) 12.5 torr, (d) 25 torr, and (e) 50 torr.²⁷

Photolytic Processes

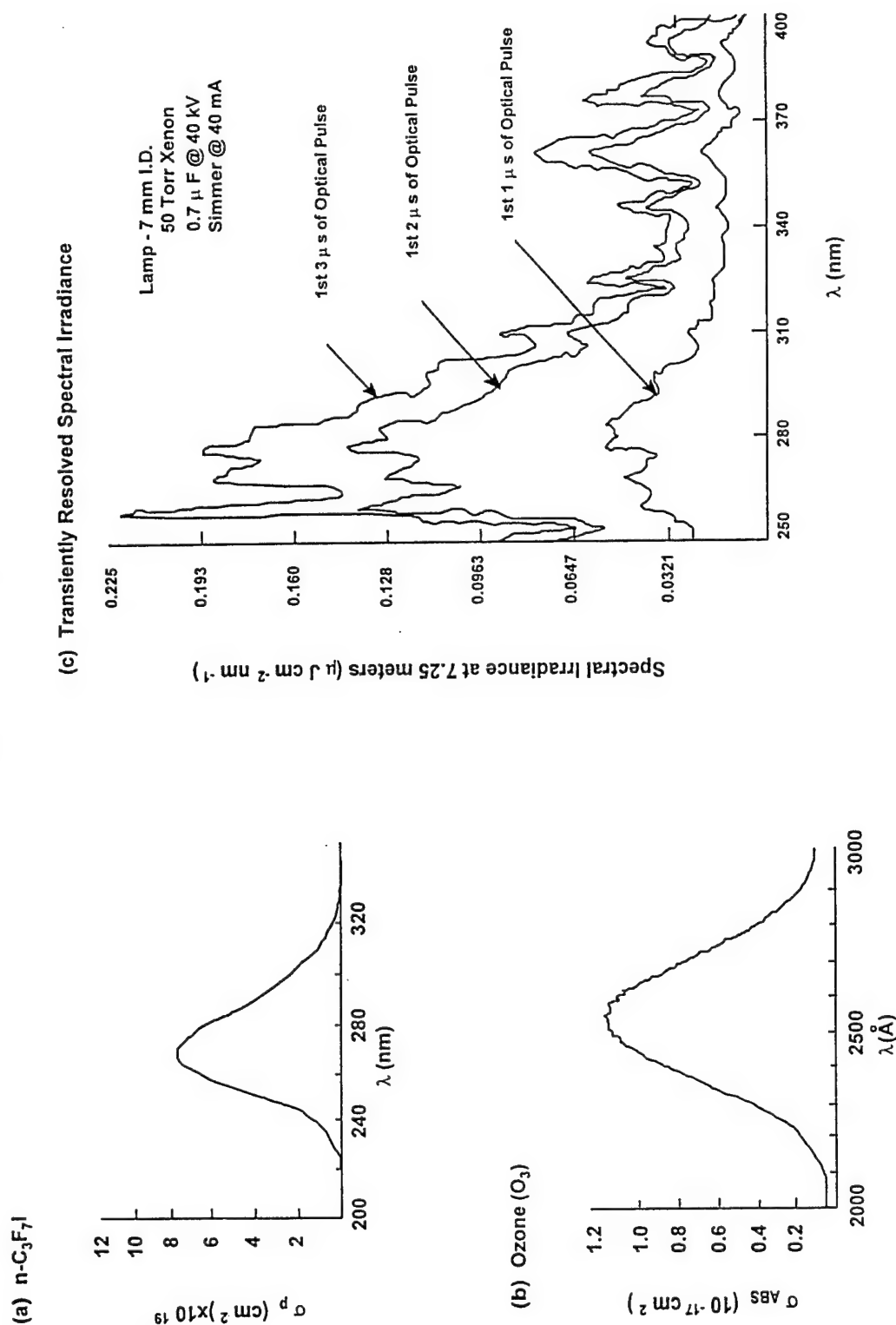


Fig. 2: Specific photolytic processes important to iodine laser, (a) photolytic cross section dependence on wavelength for production of excited iodine $5\text{-}2\text{P}_{1/2}$ atoms, (b) absorptive cross section of ozone (O_3) produced from the flashlamp UV radiation below 220 nm, and (c) transiently resolved spectral emission from pulsed flashlamp at lower pressure (50 torr)/energy (560 joules) than employed in these laser experiments.^{48,54,58} Faster onset of UV generation would be expected with the higher energies (ca 1.7 Kjoules) deposited energies into the flashlamps used here.

Pulsed PIL Device

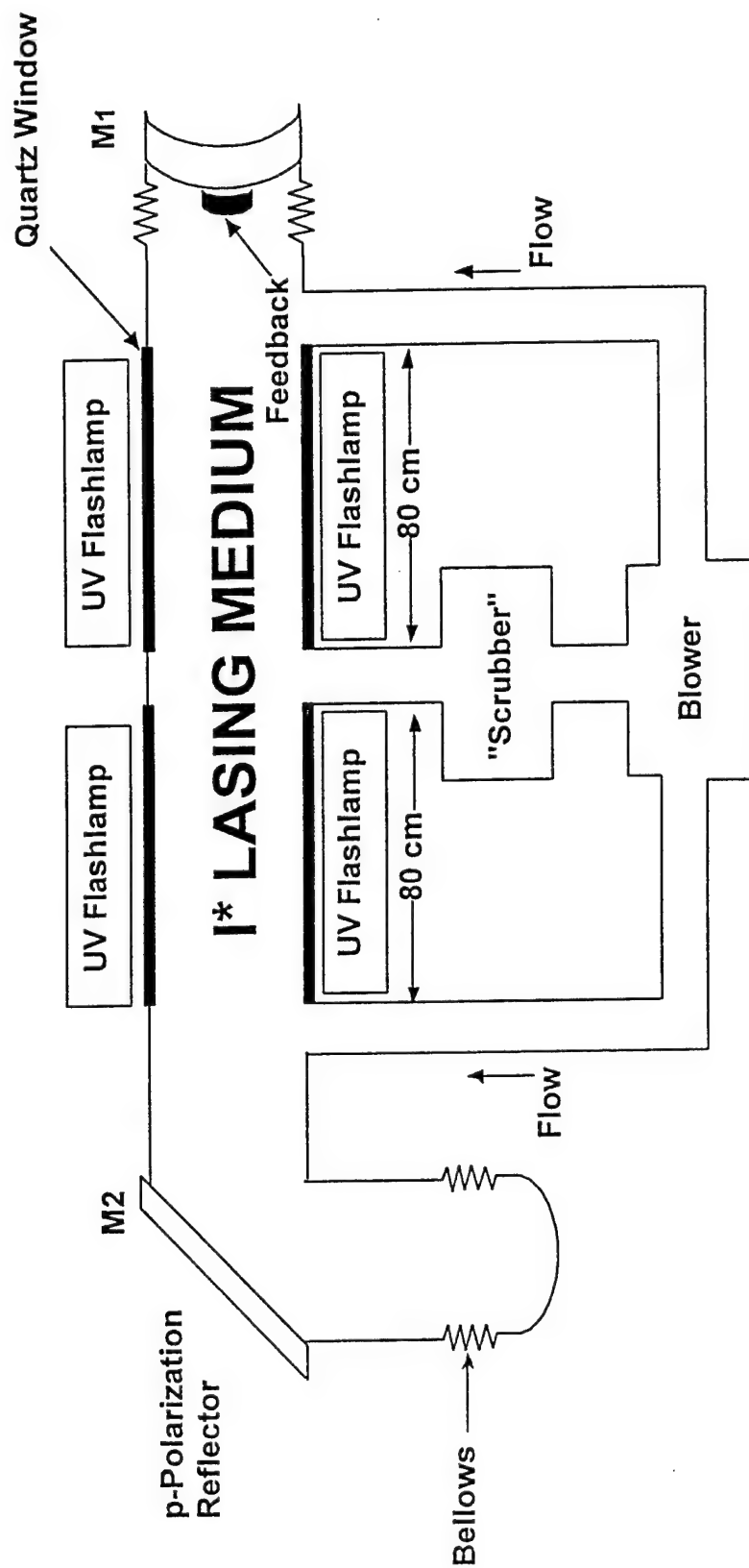


Fig. 3: Schematic for longitudinal flowing, repetitively pulsed, photolytic atomic iodine laser showing two separate gain region of 75 cm length each excited with three flashlamps from two sides and the coupling of the closed cycle laser "fuel" system including the turbo-molecular pump. On both ends of the gain region are the internally mounted mirrors of the confocal unstable resonator with a p-polarizing, 45° reflector at one end to provide polarization selectivity.

I₂ Removal System/Turbo-Molecular Pump

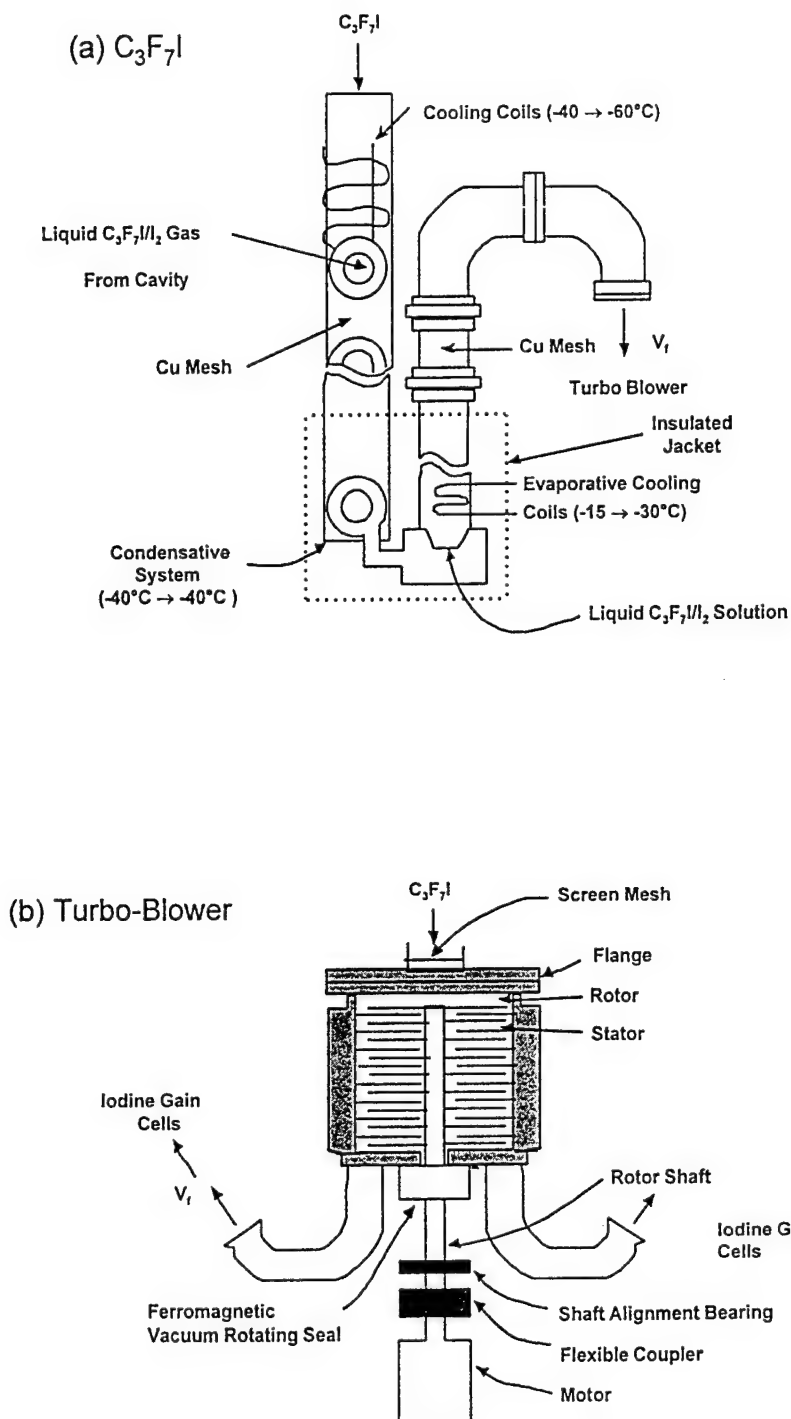


Fig. 4: C₃F₇I iodine (I₂) removal system with (a) the condensative/evaporative system and (b) turbo-molecular blower used with repetitively pulsed photolytic iodine laser.

Pulsed Flashlamp Circuitry

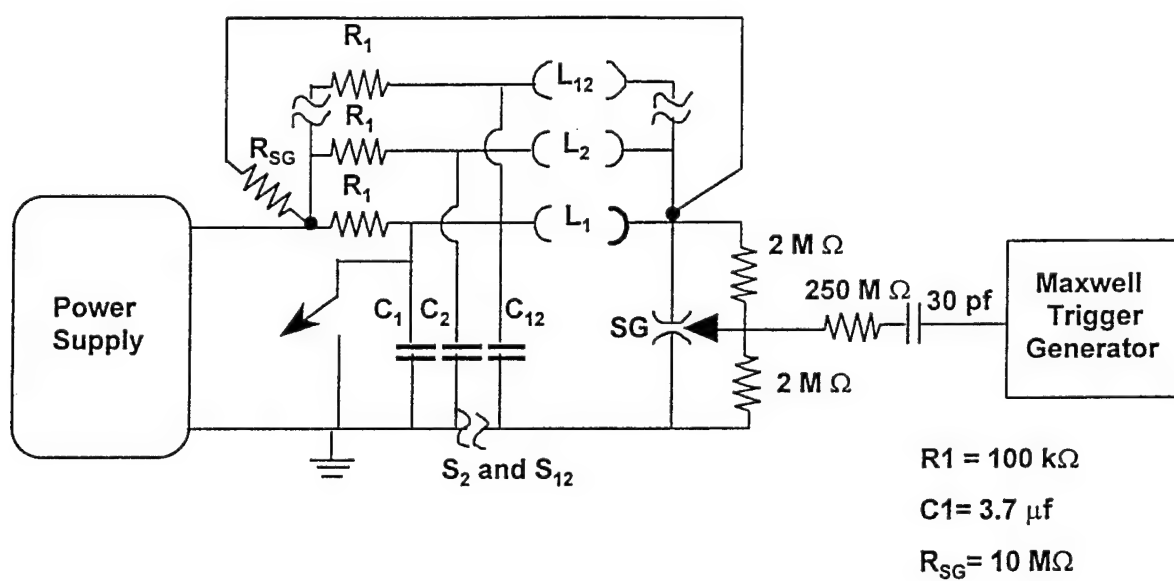
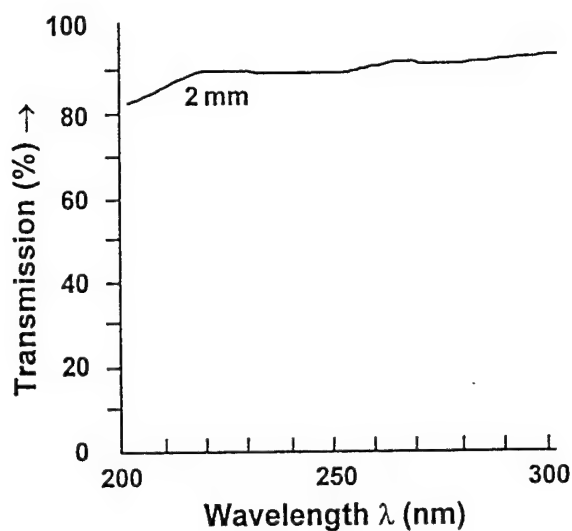


Fig. 5: Flashlamp pulse circuitry. Note, all flashlamps switched with a single spark gap to assure simultaneous firing of the UV lamps.

UV Flashlamp Transmission

(a) Low Alkali Fused Quartz Envelopes



(b) Titanium Doped Fused Quartz Envelopes

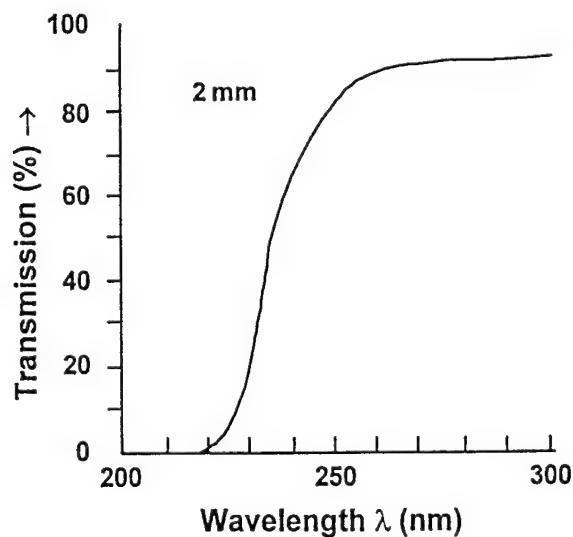


Fig. 6: Comparison of UV transmission for two types of quartz flashlamp, (a) conventional low alkali quartz tubing and (b) titanium "doped" fused quartz tubing. The near 220 nm lower cutoff for the titanium "doped" tubing gave approximately 10-15% laser improvement over the low alkali quartz flashlamps when both were water cooled.

Vapor Pressures

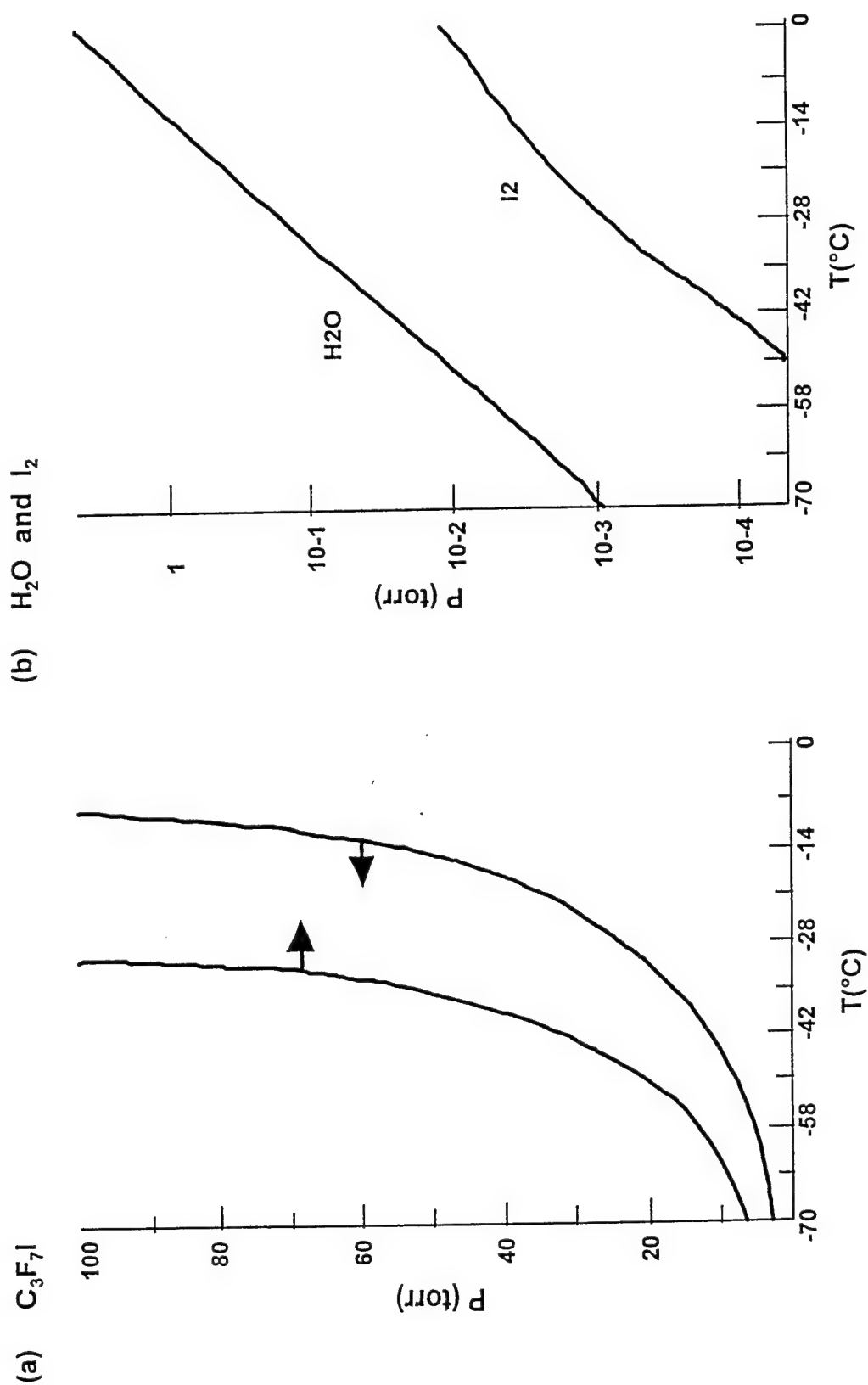


Fig. 7: Vapor pressure curves for species important in long term operation of photolytic iodine lasers, (a) C_3F_7I and (b) molecular iodine (I_2) plus water vapor (H_2O).

Integrated Laser Beam Diagnostics

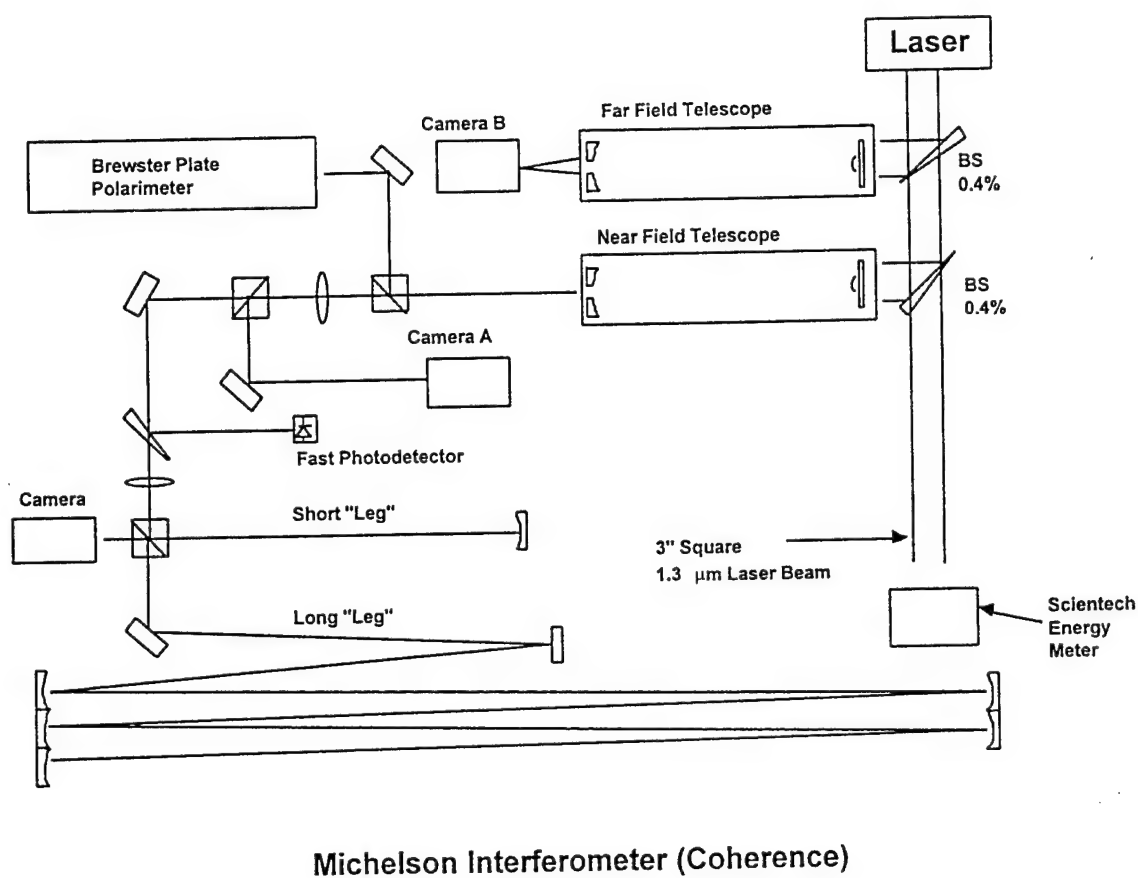


Fig. 8: Simultaneous laser beam diagnostic schematic for examining pulsed photolytic atomic iodine laser.

Detailed Laser Beam Diagnostic

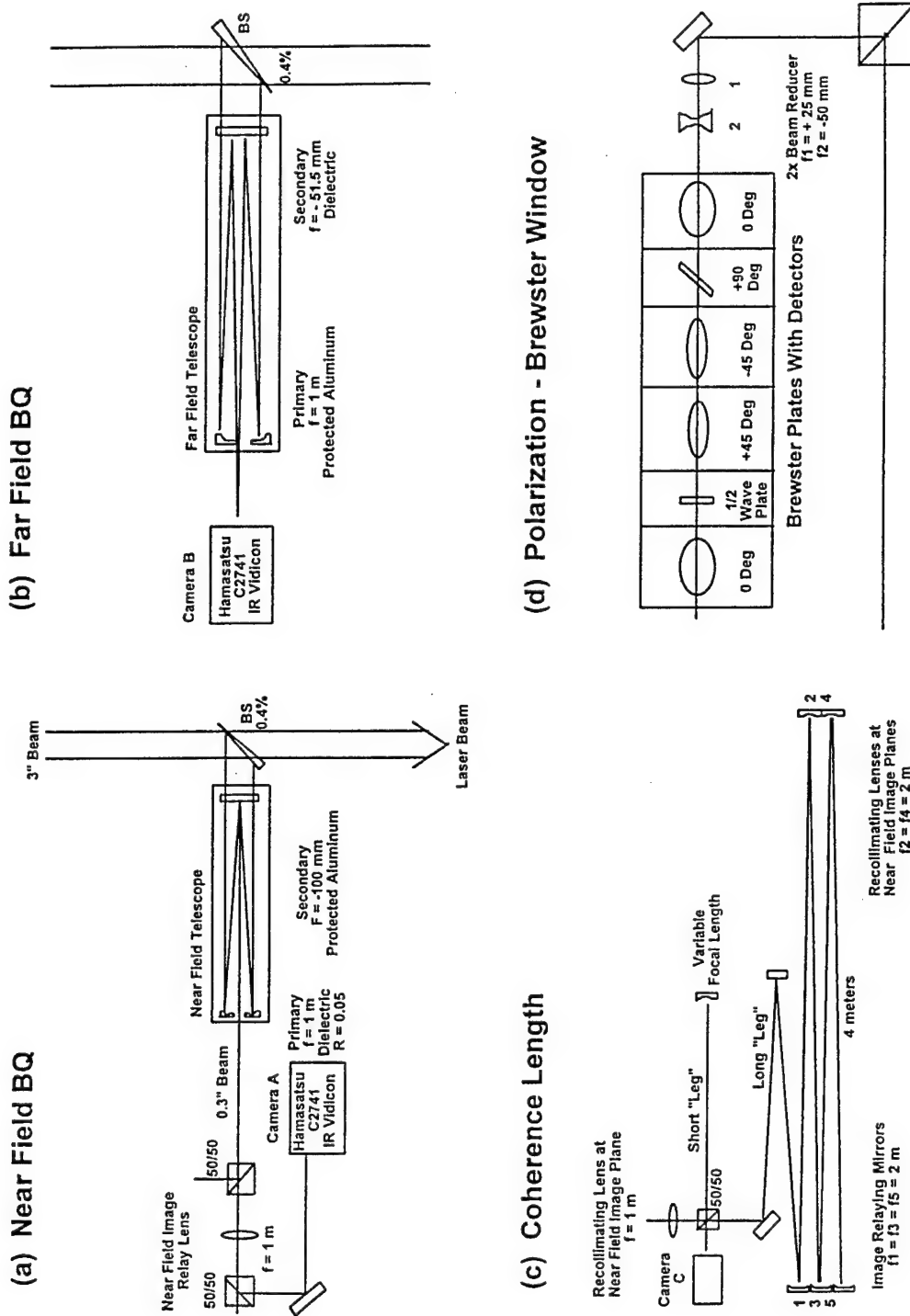


Fig. 9: Detailed schematic of laser beam diagnostics shown in Fig. 8 for pulsed photolytic atomic iodine laser, (a) laser beam quality (BQ) with telescope, (b) far-field laser beam quality with Cassegrainian telescope, (c) laser coherence length with Michelson interferometer, and (d) laser beam polarization with Brewster window arrangement.

Laser Energy vs Pressure -Stable Energy-

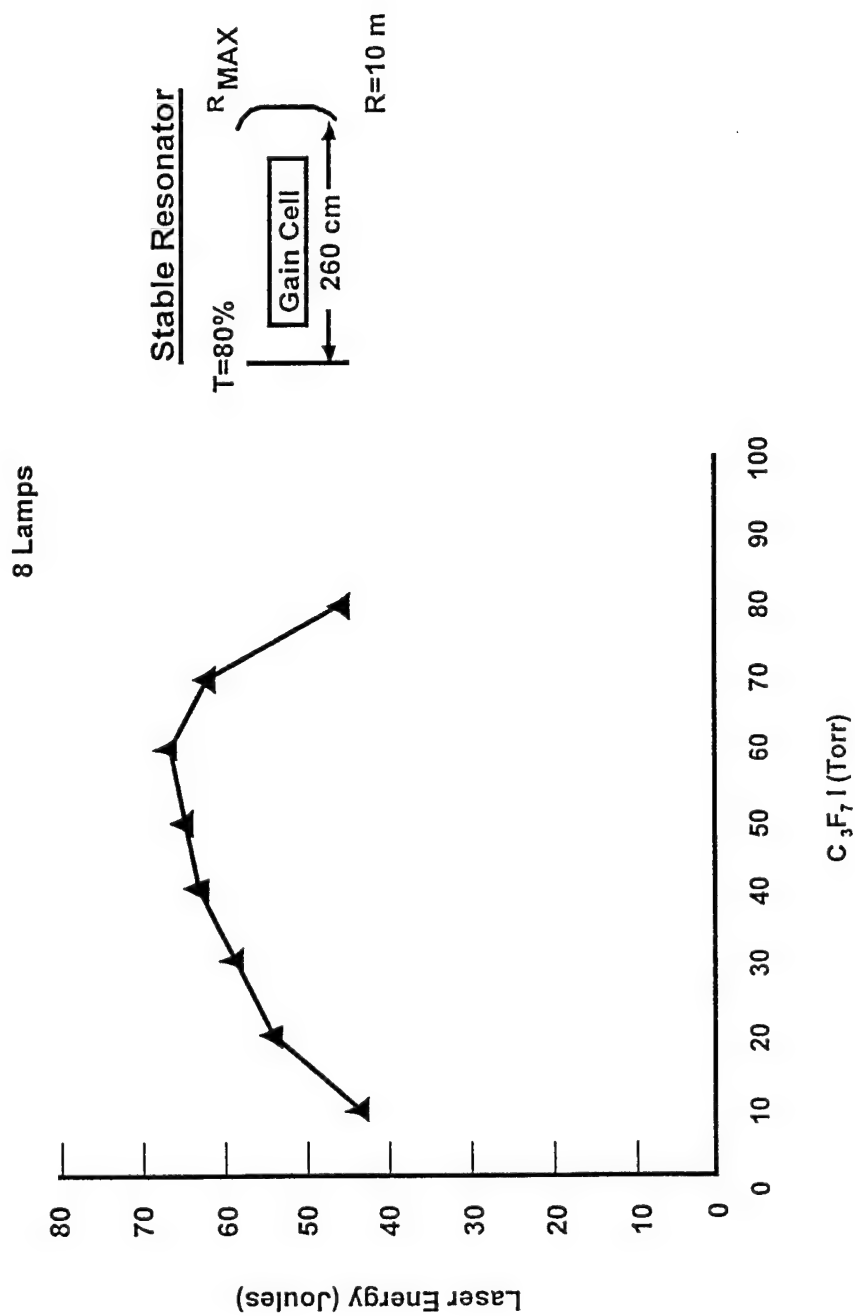


Fig. 10: Stable resonator energy performance with 80% outcoupling versus C_3F_7I pressure using 8 flashlamps with 2 lamps on each of the UV transmitting quartz lamps. Each lamp was excited with separate 3.7 μf capacitor at 30 KV. A similar curve having higher energies is obtained with 12 lamps.

Laser Energy vs Output Coupling

-Stable Resonator-

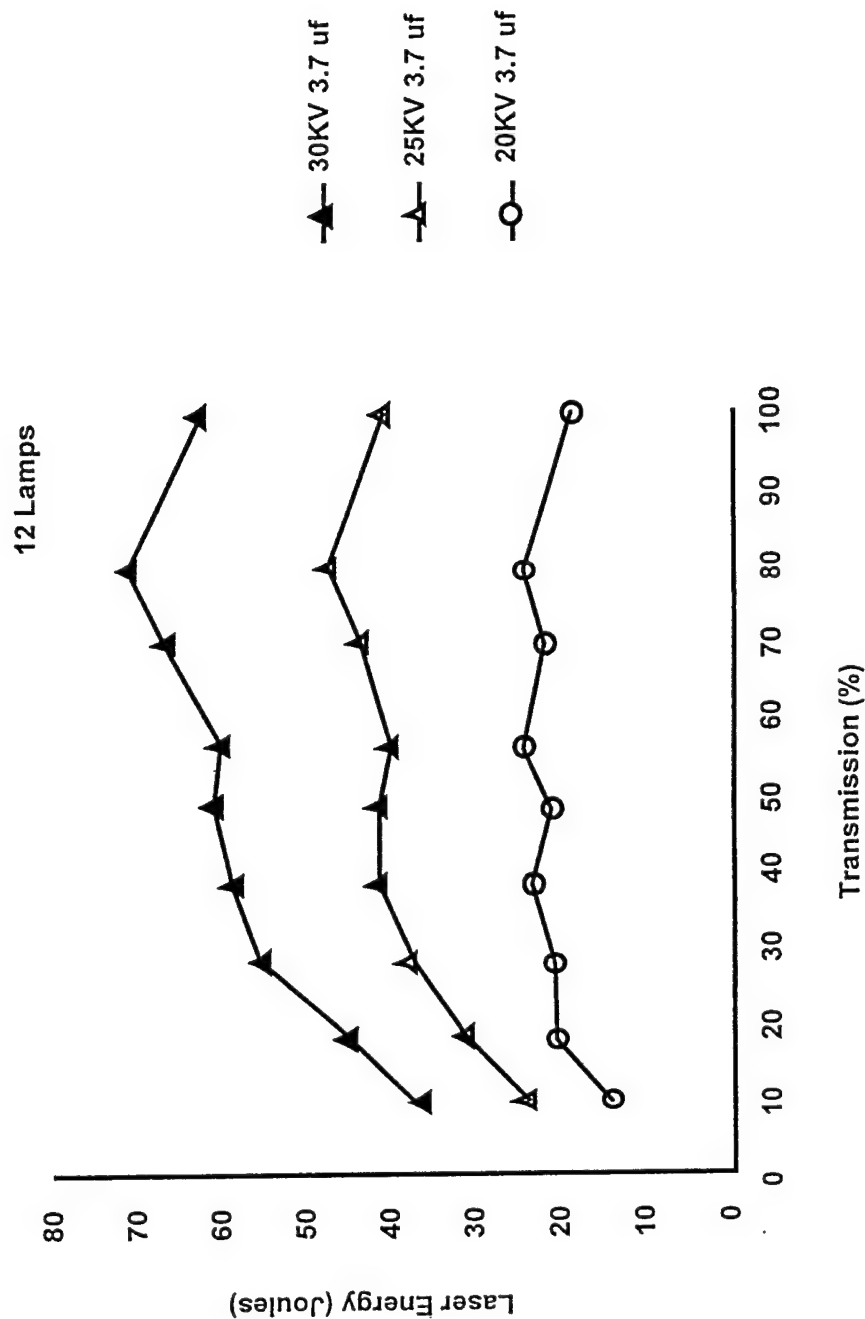


Fig. 11: Laser energy versus output coupling for 12 lamp arrangement at different flashlamp capacitor energies with an hemispherical resonator, (a) 10% coupling, (b) 20% coupling, (c) 30% coupling, (d) 39% coupling, (e) 59% coupling, and (f) 80% coupling. A 12 lamps system corresponds to 3 lamps being placed on each UV transmitting quartz window.

Laser Pulsewidth vs Output Coupling

- Stable Resonator -

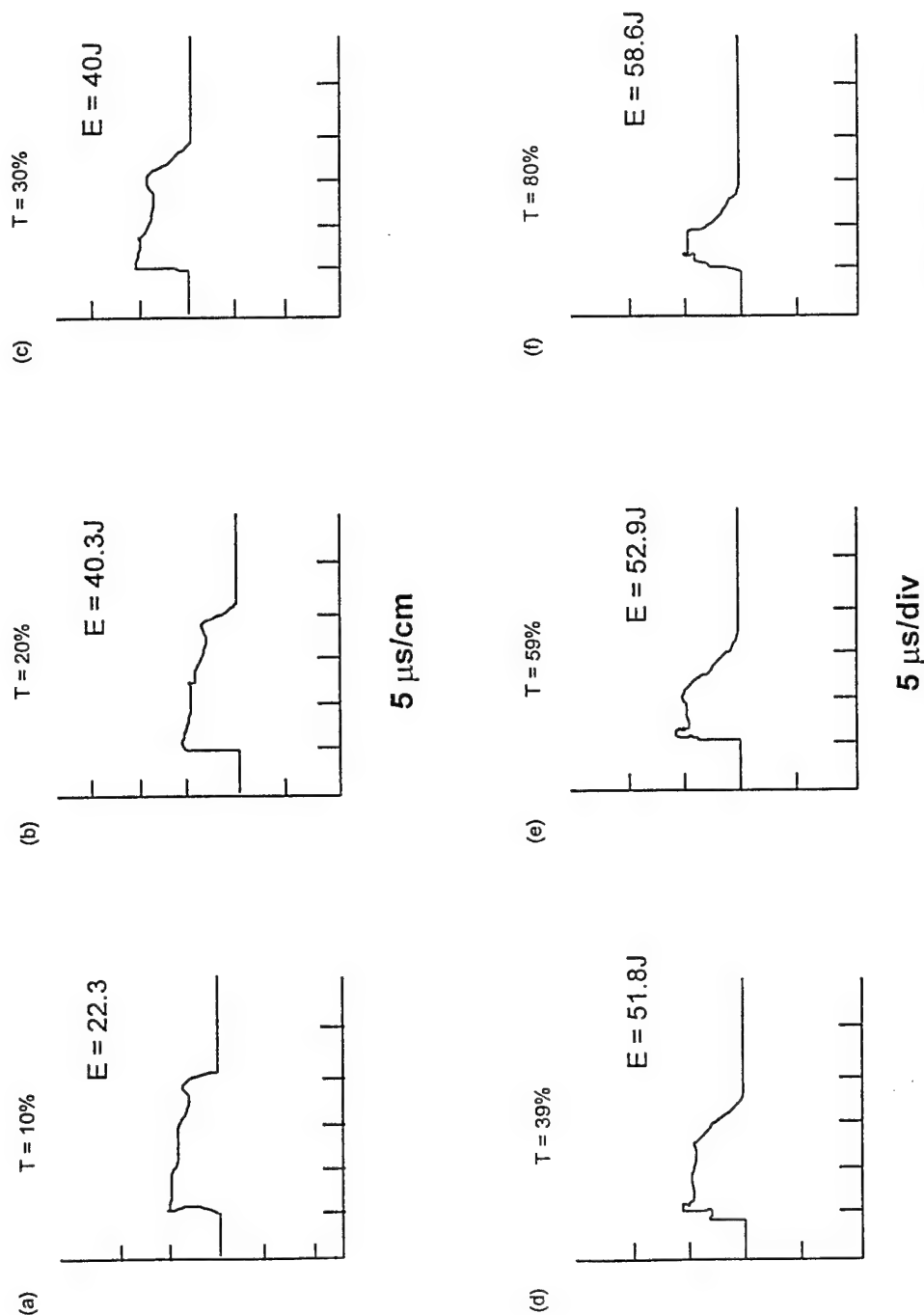


Fig. 12: Effect of output coupling on laser pulsewidth for stable resonator using 8 lamps for photolytic pumping, (a) 10% coupling, (b) 20% coupling, (c) 30% coupling, (d) 39% coupling, (e) 59% coupling, and (f) 80% coupling. Each lamp is excited with 1.7 Kjoule of energy.

Laser Energy vs Pressure

-Unstable Resonator-

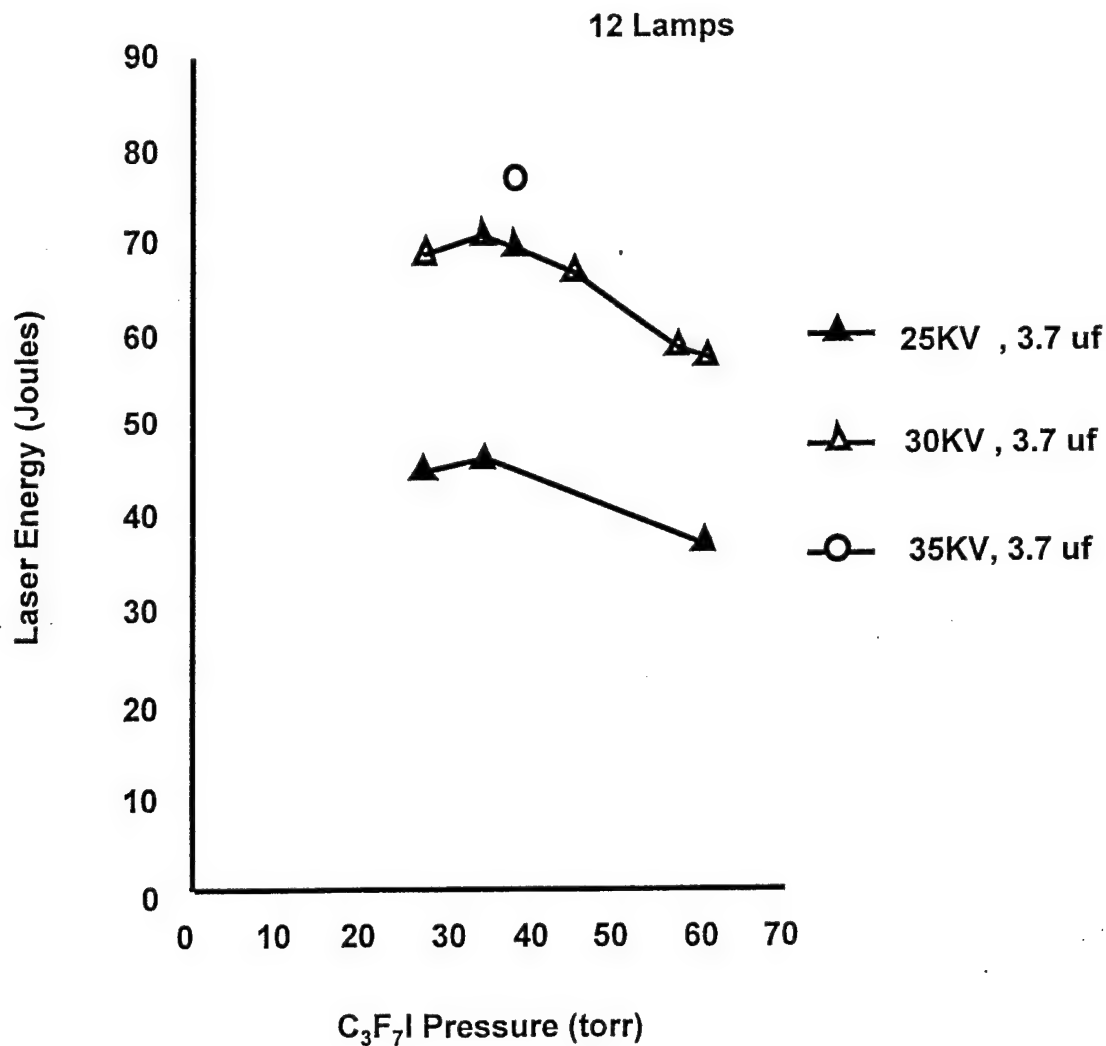


Fig. 13: Extractable laser energy from unstable resonator ($M = 3.1$) versus C_3F_7I pressure for 12 lamp arrangement at different flashlamp capacitor energies. This magnification corresponds to a geometrical output coupling of 89%. A 12 lamps system corresponds to 3 lamps being placed on each UV transmitting quartz window.

Laser Temporal Behavior Relation to Flashlamp Current

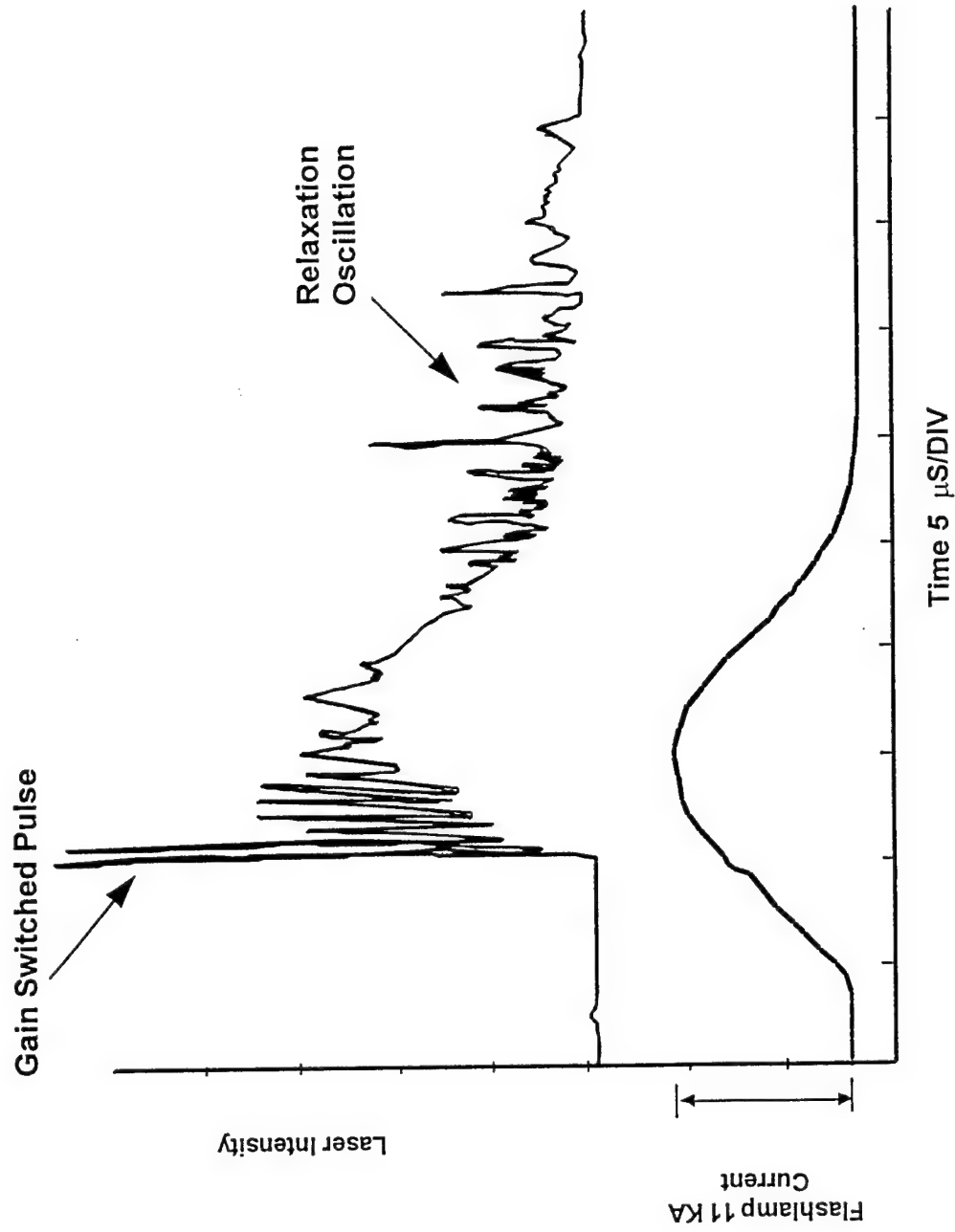


Fig. 14: Comparison of the transient behavior of laser signal with flashlamp current for $M = 3$ confocal unstable resonator as shown in Fig. 3. The $3.7 \mu\text{f}$ capacitors were charged to 30 KV giving stored energies ca 1.7 Kjoules.

Small Signal Gain

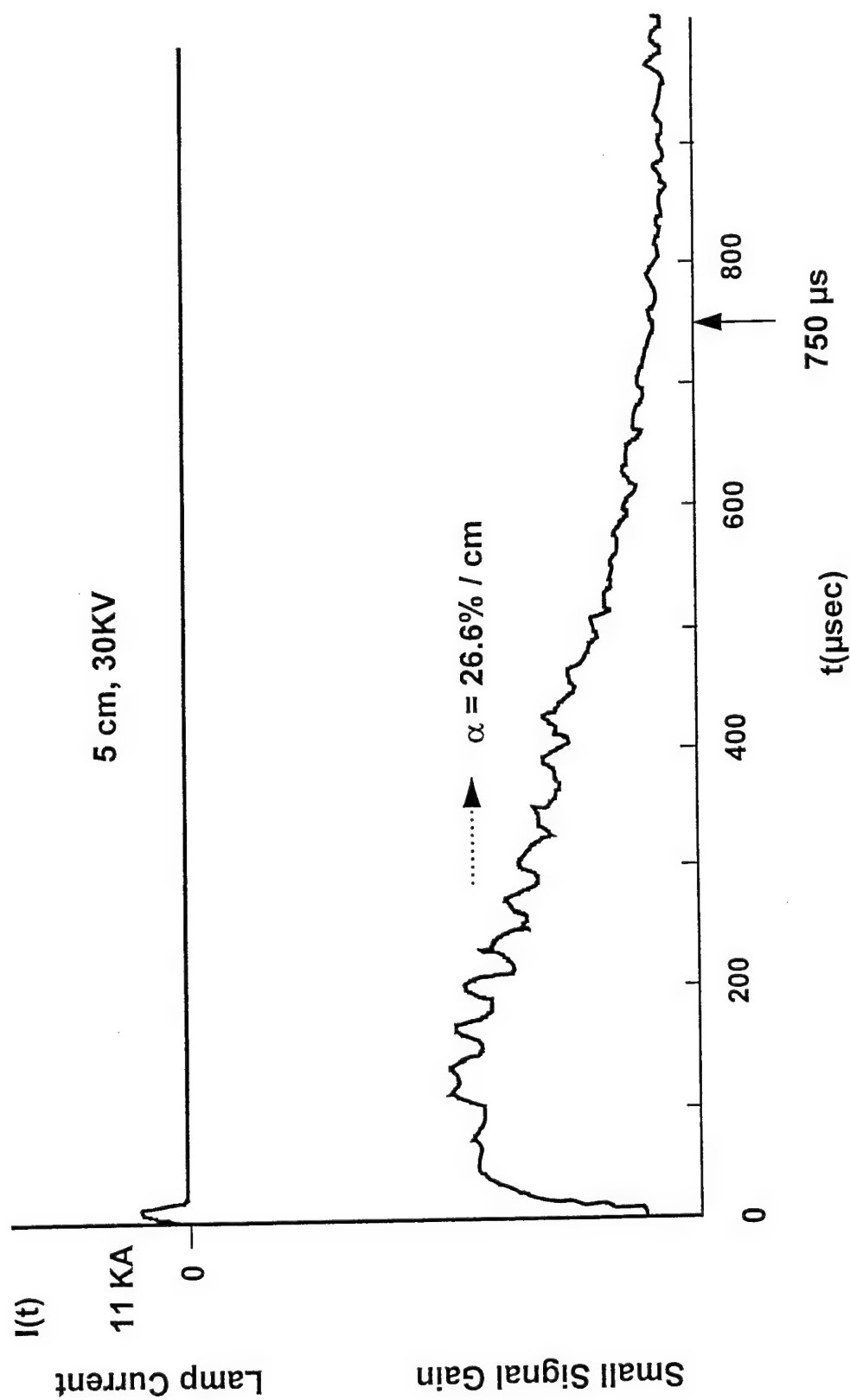


Fig. 15: Small Signal Gain Coefficient for pulsed iodine gain medium at 40 torr and 3.7 μf capacitors charged to 30 KV flashlamps over a 5 cm gain path length.

Table I: Atomic Iodine Hyperfine Transition Characteristics

Transition $F' \rightarrow F''$ ^(a)	Wavelength ^(b)		A-coefficients ^(c) (sec^{-1})
	$k(\text{cm}^{-1})$	$\lambda(\mu\text{m})$	
2-3	7602.6202	1.315336	1.76
2-2	7602.6858	1.315325	2.20
2-1	7602.7105	1.315320	1.69
3-4	7603.1385	1.315246	3.67
3-3	7603.2794	1.315222	1.54
3-2	7603.3450	1.315211	0.44

^a F' is upper state quantum number while F'' refers to lower state quantum number

^b Ref. 22

^c Refs. 23-24. Values calculated as shown in Ref. 27.

A comparison of the A-coefficients listed in Table I with the theoretical values of Ref. 11 reveals the tabular values are smaller. For example, Zuev²³ gives 5 sec^{-1} for the 3-4 transition versus the 3.67 sec^{-1} of Table I. These tabular values were determined by averaging the absolute magnitude results of Derwent and Thrush²⁴ and Zuev²³ and then multiplying that value (11.3 sec^{-1}) by the relative hyperfine transition values of Zuev²³ as previously described in Ref. 27. Listing the values in Table I is not meant to state these A-coefficient values are absolutely correct, but they are given as such to retain consistency with the anomalous dispersion results of Ref. 27 and the gain results of Fig. 1-c,e.

Table II: Mean Free Path Lengths for Various Pressures of C_3F_7I

n- C_3F_7I Pressure (torr) ^(a)	Mean Free Path Length - l_p (cm)
10	7.67
20	3.83
30	2.56
35	2.19
40	1.92
45	1.70
50	1.53
60	1.28
70	1.10

^a All calculations made assuming gas temperature of 23°C

Table III: Critical Kinetic Processes for Pulsed Photolytic Iodine Laser at 1.315 μM .

RI represents $n\text{-C}_3\text{F}_7\text{I}$.

<u>Process</u>	<u>Rate Coefficient</u> ^(a)	<u>Reference</u>
1. $\text{RI} + h\nu_{\text{pump}} \rightarrow \text{R} + \text{I}$	$\sigma_{\text{p}}(\text{max}) = 7.8 \times 10^{-19} \text{cm}^2$	34-36
2. $\text{I}^* \rightarrow \text{I} + h\nu_{\text{rad}}$	$A = 7.7 \text{ sec}^{-1}$	23,24
3. $\text{I}^* \rightarrow \text{I} + h\nu_{\text{laser}}$	$\sigma_{\text{se}} = 5.5 \times 10^{-18} \text{cm}^2 \text{ (b)}$	27
4. $\text{I} + \text{R} \rightarrow \text{RI}$	4.7×10^{-11}	37-41
5. $\text{I}^* + \text{R} \rightarrow \text{RI}$	7.9×10^{-13}	37-41
6. $\text{R} + \text{R} \rightarrow \text{R}_2$	1.3×10^{-12}	37-41
7. $\text{I}^* + \text{RI} \rightarrow \text{I} + \text{RI}$	2.8×10^{-16}	37-41
8. $\text{I}^* + \text{O}_2 \rightarrow \text{I} + \text{O}_2(^1\Delta_g)$	2.5×10^{-11}	42-44
9. $\text{I}^* + \text{H}_2\text{O} \rightarrow \text{I} + \text{H}_2\text{O} + \text{heat}$	9.6×10^{-13}	45
10. $\text{I}^* + \text{N}_2 \rightarrow \text{I} + \text{N}_2 + \text{heat}$	5.2×10^{-17}	42-43
11. $\text{I}^* + \text{I} + \text{RI} \rightarrow \text{I}_2 + \text{RI}$	3.8×10^{-31}	37,46
12. $\text{I}^* + \text{I} + \text{I}_2 \rightarrow 2\text{I}_2$	3.7×10^{-30}	47
13. $\text{I}^* + \text{I}_2 \rightarrow \text{I} + \text{I}_2 + \text{heat}$	9.9×10^{-12}	42-43

^a Rate coefficients have dimensions $(\text{cm}^3/\text{molecules})^n / \text{sec}$ where $n=1$ for two body processes and $n=2$ for three body processes.

^b Evaluated assuming only Doppler broadening ($T=300^\circ\text{K}$) - Ref. 27. At higher pressures, the effects of pressure broadening on σ_{se} must be included as shown in Table 3 of Ref. 27.

LIST OF REFERENCES

1. G. Brederlow, E. Fill, and K. J. Witte, *The High-Power Iodine Laser* (Springer-Verlag Berlin Heidelberg, New York, 1983).
2. K. T. Witte, G. Brederlow, K. Eidmann, R. Volk, E. Fill, K. Hohla, and R. Roadmann, "Photodissociation Lasers For Controlled Thermonuclear Fusion", *Springer Series Opt. Sci.*, 9, pp. 142-197, 1978.
3. A. J. DeMaria and C. J. Ultee, "High-Energy Atomic Iodine Photodissociation Laser", *Appl. Phys. Lett.*, 9, pp. 67-69, 1966.
4. N. G. Basov and V. S. Zuev, "Short-Pulse Iodine Laser", *Il Nuovo Cimento*, 31, pp. 29-32, 1976.
5. H. J. Baker, T. A. King, and W. G. McNaught, "The Multi-Atmospheric Pressure Operation of a Gain-Switched Iodine Laser", *J. Phys. D: Appl. Phys.*, 12, 997-1004, 1979.
6. H. J. Baker and T. A. King, *Laser Advances and Applications*, edited by B. S. Wherrett (Wiley, New York, 1980), p.80.
7. S. B. Kormer, "Photolysis Lasers for Controlled Nuclear Fusion", *Izvestiya Akademii Nauk USSR: Ser. Fizz.*, 44, 2002-2017, 1980.
8. O. P. Judd, C. R. Jones, and W. C. Davis, "High Energy Atomic Iodine Laser", LA-10946-MS, April, 1987, Los Alamos National Laboratory, Los Alamos, N.M.
9. C. R. Jones and W. C. Davis, "Optical Properties of Explosive-Driven Shock Waves in Noble Gases", LA-9475-MS, 1982.
10. P. O. Andreeva, G. N. Birich, I. I. Sobelman, V. N. Sorokin, and I. I. Struk, "Continuously Pumped Continuous-Flow Iodine Laser", *Sov. J. Quantum Electron.*, 7, pp. 1230-1234, 1977.
11. K. J. Witte, P. Burkhar, and H. R. Luthi, "Low-pressure Mercury Lamp Pumped Atomic Iodine Laser of High Efficiency", *Opt. Comm.*, 28, pp. 202-206, 1979.
12. V. Y. Zalesskii, E. S. Ershov, A. M. Kokushkin, and S. S. Polikarpov, "Continuous-Wave Operation of a Photodissociation Iodine Laser", *Sov. J. Quantum Electron.*, 11, pp. 498-502, 1981.
13. L. A. Schlie and R. D. Rathge, "Long Operating Time cw Atomic Iodine Laser at 1.315 Microns", *IEEE J. of Quant. Electr.*, 20, pp. 1187-1196, 1984.
14. L. A. Schlie and R. D. Rathge, "Transverse Flow, cw Atomic Iodine Laser at 1.315 μm ", *J. of Appl. Phys.*, 63, pp. 5664-5667, 1988.

15. L. A. Schlie and R. D. Rathge, "Closed-Cycle Gaseous Alkyl Iodine (C_3F_7I) Supply System", *Rev. Sci. Instrum.*, 55, pp. 482-485, 1984.
16. W. Fuss and I. Hohla, "A Closed Cycle Iodine Laser", *Opt. Comm.*, 18, pp. 427-430, 1976.
17. S. D. Herrera, L. A. Schlie, and S. A. Richert, "Scaled-up Production of $n-C_3F_7I$ Photolytic Laser 'Fuel'", *Rev. of Scient. Instrum.*, 59, pp. 2386-2389, 1988.
18. I. M. Belousova, V.M. Kiselev, and V.N. Kurzenkov, "Induced Emission Spectrum of Atomic Iodine Due to the Hyperfine Structure of the Transition $^2P_{1/2} - P_{3/2}$ (7600 cm^{-1})", *Opt. Spectrosc.*, 33, pp. 112-114, 1972.
19. R. M. Eisberg, *Fundamentals of Modern Physics* (John Wiley & Sons, New York 1961), pp. 449-452.
20. V. Jaccarino et al., "Hyperfine Structure of I^{127} . Nuclear Magnetic Octupole Moment," *Phys. Rev.*, 94, pp. 1798-1799, 1954.
21. E. Luc-Koenig, C. Morillon, and J. Verges, "Etude Experimentale et Theorique de la Ligne Atomique", *Phys. Scr.*, 12, pp. 199-204, 1975.
22. R. Engleman, Jr., R. A. Keller, and B. A. Palmer, "Hyperfine Structure and Isotope Shift of the $1.3\text{ }\mu\text{m}$ Transition of I^{129} ", *Appl. Opt.*, 19, pp. 2767-2770, 1980.
23. V.S. Zuev, V. A. Katulin, V. Yu Nosach, and O. Yu. Nosach, "Investigation of the Luminescence Spectrum of Atomic Iodine ($^2P_{1/2} - ^2P_{3/2}$) Laser Transition", *Sov. Phys. JETP*, 35, pp. 870-873, 1972.
24. R. S. Derwent and B.A. Thrush, "The Radiative Lifetime of the Metastable Iodine Atom $I(^5P_{1/2})$ ", *Chem. Phys. Lett.*, 9, pp. 591-592, 1971.
25. A. Yariv, *Introduction to Optical Electronics*, 3rd Ed. (Holt, Rinehart, & Winston, New York, 1976), pp 335-339.
26. D. C. O'Shea, W. R. Callen, and W. T. Rhodes, *An Introduction to Lasers and Their Applications* (Addison-Wesley, Reading, MA, 1977), pp. 28-32.
27. L. A. Schlie, "Anomalous Dispersion Effects in Low-Pressure Atomic Iodine Lasers at $1.315\text{ }\mu\text{m}$ ", *J. of Opt. Soc. Amer.*, 71, pp.1080-1093, 1981.
28. W. Fuss and K. Hohla, "Pressure Broadening of $1.3\text{ }\mu\text{m}$ Iodine Laser Line", *Z. Naturforsch, Teil A*, 31, pp. 569-577, 1976.

29. T.D. Padrick and R.E. Palmer, "Pressure Broadening of the Atomic Iodine $5^2P_{1/2}$ - $5^2P_{3/2}$ Transition," J. Chem. Phys., 62, pp. 3350-3351, 1975.
30. D. K. Neumann, P. K. Clark, R. F. Shea, and S. J. Davis, " O_2 Pressure Broadening of Iodine $^2P_{1/2}$ - $^2P_{3/2}$ Transition", J. of Chem. Phys., 79, pp. 4680-4682, 1983.
31. R. Engelman, Jr., B. A. Palmer, and S. J. Davis, "Transition Probability and Collision Broadening of the 1.3 Micron Transition of Atomic Iodine", J. of Opt. Soc. Am., 73, pp. 1585-1589, 1983.
32. For a discussion of the existence of only one longitudinal mode in a homogeneously broadened gain medium, see A. E. Siegman, Lasers (University Science Books, Mill Valley, CA, 1986), pp. 462-3.
33. L. A. Schlie and R. D. Rathge, "Long Coherence Length for cw Photolytic Atomic Iodine Laser at 1.315 μ m", Opt. Lett., 16, pp. 1007-1009, 1991.
34. J. E. Smedley and S. R. Leone, "Relative Quantum Yields of $I^*(^2P_{1/2})$ in the Tunable Laser UV Photodissociation of *i*-C₃F₇I and *n*-C₃F₇I: Effect of Temperature and Exiplex Emission", J. Chem. Phys., 79, pp. 2687-2695, 1983.
35. J. S. Cohen and O. P. Judd, "High-Energy Optically Pumped Iodine Laser: I. Kinetics in a Optically Thick Medium", Phys. Rev., 55, pp. 2659-2671, 1983.
36. J. S. Cohen and O. P. Judd, "Transport of Broadband Radiation Through a Nonlinear Dispersive Medium", Phys. Rev., 55, pp. 3146-3157, 1983.
37. F. E. Beverly, III., "Pressure-Broadened Iodine Laser Amplifier Kinetics and a Comparison of Diluent Effectiveness", Opt. Comm., 15, pp. 204-208, 1975.
38. V. Y. Zalesskii and E. I. Moskalev, "Optical Probing of Photodissociative Laser", Sov. Phys. JETP, 30, pp. 1019-1023, 1970.
39. V. Y. Zalesskii and A. A. Venediktov, "Mechanism of Generation Termination at the $5^2P_{1/2}$ - $5^2P_{3/2}$ Transition in Iodine", Sov. Phys. JETP, 28, pp. 1104-1107, 1969.
40. I. M. Belousove, N. G. Gorshkov, O. B. Danilov, V. Y. Zalesskii, and I. L. Yachnev, "Accumulation of Iodine Molecules in Flash Photolysis of CF₃I and *n*-C₃F₇I Vapor", Sov. Phys. JETP, 38, pp. 254-257, 1974.
41. V. Y. Zalesskii, "Analytic Estimate of the Maximum Duration of Stimulated Emission for a CF₃I Photodissociation Laser", Sov. J. Quant. Electr., 4, pp. 1009-1014, 1975.

42. J. J. Deakin and D. Husain, "Temperature Dependence of Collisionally Induced Spin Orbit Relaxation of Electronically Excited Iodine Atoms, $I(5^2P_{1/2})$ ", Chem. Soc., Faraday II, 68, pp. 1603-1612, 1972.
43. D. H. Burde, R. A. McFarlane, and J. R. Wiesenfeld, "Collisional Quenching of Excited Iodine Atoms $I(5p^5 2P_{1/2})$ by I_2 ", Chem. Phys. Lett., 32, pp. 296-299, 1975.
44. R. G. Derwent and B. A. Thrush, "Excitation of Singlet Molecular Oxygen", J. Chem. Soc. Faraday II, 68, pp. 720-724, 1972.
45. A. J. Grimley and P. L. Houston, "Electronic to Vibrational Energy Transfer from $I(5^2P_{1/2})$. II. H_2O , HDO , and D_2O ", J. of Chem. Phys., 69, pp. 2339-2346, 1978.
46. S. V. Kuznetsova and A. I. Maslov, "Investigations of the Reactions of Atomic Iodine in a Photodissociation Laser Using $n-C_3F_7I$ and $i-C_3F_7I$ ", Sov. J. Quant. Electr., 3, pp. 468-471, 1974.
47. J. A. Blake and G. Burns, "Kinetics of Iodine Atom Recombination Between 300 and 1165°K", J. of Chem. Phys., 54, pp. 1480-1486, 1971.
48. J. H. Goncz and P. B. Newell, "Spectra of Pulsed and Continuous Xenon Discharges", J. of Opt. Soc. Am., 56, pp. 87-92, 1966.
49. J. L. Emmett and A. L. Schawlow, "Enhanced Ultraviolet Output from Double-Pulsed Flashlamps", Appl. Phys. Lett., 2, pp. 2601-2608, 1963.
50. J. L. Emmett, A. L. Schawlow, and E. H. Weinberg, "Direct Measurement of Xenon Flashtube Opacity", J. of Appl. Phys., 35, pp. 2601-2604, 1964.
51. J. H. Goncz, "Resistivity in Xenon Plasmas", J. of Appl. Phys., 36, pp. 742-743, 1965.
52. J. P. Markiewicz and J. L. Emmett, "Design of Flashlamp Driving Circuits", IEEE J. of Quant. Electr., 2, pp. 707-711, 1966.
53. P. A. Lovoi, "Flashlamp Technology for Pulsed Lasers", Advances in Laser Technology (Emphasizing Gaseous Lasers), SPIE 78, 13, pp. 2-9, 1978.
54. M. P. Vanyukov and A. A. Mak, "High-Intensity Pulsed Light Sources", Sov. Phys., 66, pp. 137-155, 1958.
55. L. K. Gavrilina, V. Y. Karpov, Y. S. Leonov, V. A. Sautkin, and A. A. Filyukov, "Selective Pumping Effect of a Photodissociative Laser", JETP, 35, pp. 258-259, 1972.
56. K. M. Swift, L. A. Schlie, and R. D. Rathge, "Dispersion of Gases in Atomic Iodine Lasers at 1.315 μM ", Appl. Opt., 27, pp. 4377-4384, 1988.

57. *Physics of Color Centers*, Ed. W. Beall Fowler (Academic Press, New York, 1968).
58. ILC Technology Corp., 164 Commercial Street, Sunnyvale, CA and see ILC Technical Bulletin 3, "An Overview of Flashlamps and cw Arc Lamps" and "Linear Flashlamps" Technical Bulletin.
59. R. W. Ditchburn and P. A. Young, "The Absorption of Molecular Oxygen Between 1850 Å and 2500 Å", *J. Atmos. Terr. Phys.*, 24, pp. 127-136, 1962.
60. A. J. Blake, J. H. Carver, and G. N. Haddad, "Photo-Absorption Cross Sections of Molecular Oxygen Between 1250 Å and 2350 Å", *J. Quant. Spectr. Rad. Transf.*, 6, pp. 451-456, 1966.
61. R. E. Palmer, T. D. Padrick, and R. B. Pettit, "Evaluation of Flashlamp Reflectors for the Atomic Iodine Photodissociation Laser", *J. of Appl. Phys.*, 48, pp. 3125-3126, 1977.
62. J. B. Morris, R. A. Stinchcombe, M. D. Gray, and D. H. Logsdail, "Removal of Iodine Vapour from Air by Metallic Copper", United Kingdom Atomic Energy Research Establishment (AERE), October, 1962, Harwell, England.
63. R. M. Olson, *Essential of Engineering Fluid Mechanics* (International Textbook Company, Scranton, PA, 1962), see Chapt. 14, pp. 344-365.
64. K. Raj, "Testing Magnetic Fluid Seals", *Vacuum Technology, Industrial Research/Development*, pp. 115-119, March 1979.
65. K. Raj and C. Reiser, "Magnetic-Fluid Seals", *Laser Focus*, pp. 56-59, April, 1979.
66. W. W. Rigrod, "Gain Saturation and Output Power of Optical Masers", *J. of Appl. Phys.*, 34, pp. 2602-2609, 1963.
67. W. W. Rigrod, "Saturation Effects in High Gain Lasers", *J. of Appl. Phys.* 36, pp. 2487-2490, 1965.
68. T. A. Cool, "Power and Gain Characteristics of High Speed Flow Lasers", *J. of Appl. Phys.*, 40, pp. 3563-3573, 1969.
69. W. W. Rigrod, "Homogeneously Broadened cw Lasers with Uniform Distributed Loss", *IEEE J. of Quant. Electr.*, 14, pp. 377-383, 1978.
70. A.E. Siegman, "Unstable optical resonators for laser applications", *Proc. IEEE*, 53, pp. 277-287, 1965.
71. A.E. Siegman and R. Arrathoon, "Modes in Unstable Optical Resonators and Lens Waveguides", *IEEE J. Quantum Electron*, 3, pp. 156-164, 1967.

72. A.E. Siegman, "Stabilizing Output with Unstable Resonators", *Laser Focus* 7, pp. 42-47 (1971).
73. W. F. Krupke and W. R. Sooy, "Properties of an Unstable Confocal Resonator CO₂ Laser System", *IEEE J. of Quant. Electr.*, 5, pp. 575-586, 1969.
74. J. Tellinghuisen, "Resolution of the Visible-Infrared Absorption Spectrum of I₂ into Three Contributing Transitions", *J. of Chem. Phys.*, 58, pp. 2821-2834, 1973.
75. Ref. 32, pp. 954-969.
76. J. Goldhar and M. A. Hensian, "Large-Aperture Electrooptical Switches with Plasma Electrodes", *IEEE J. of Quant. Electr.*, 22, pp. 1137-1147, 1986.
77. J. Goldhar and M. A. Hensian, "Electro-Optical Switches with Plasma Electrodes", *Opt. Lett.*, 9, pp. 73-75, 1984.
78. M. A. Hensian and J. Goldhar, "Demonstration of Electro-Optical Switching at the 26 cm x 26 cm Aperture Using Plasma Electrodes", *Opt. Lett.*, 9, pp. 516-518, 1984.
79. M. A. Hensian, J. Goldhar, and R. A. Haas, "Electro-Optic Harmonic Conversion Switch for Large-Aperture Multipass Laser Systems", *Opt. Lett.*, 9, pp. 365-367, 1984.
80. D. Eimerl, "Thermal Aspects of High-Average-Power Electro-Optic Switches", *IEEE J. of Quant. Electr.*, 23, pp. 2238-2251, 1987.

DISTRIBUTION LIST

AUL/LSE

Bldg 1405 - 600 Chennault Circle

Maxwell AFB, AL 36112-6424 1 cy

DTIC/OCP

8725 John J. Kingman Rd, Suite 0944

Ft Belvoir, VA 22060-6218 2 cys

AFSAA/SAI

1580 Air Force Pentagon

Washington, DC 20330-1580 1 cy

PL/SUL

Kirtland AFB, NM 87117-5776 2 cys

PL/HO

Kirtland AFB, NM 87117-5776 1 cy

Official Record Copy

PL/LIDD/Dr. Vern Schlie

Kirtland AFB, NM 87117-5776 8 cys